gels

MDPI

Review

Multiscale Structure–Property Relationships in Food Gels: From Molecular Interactions to Food Applications

Sergio A. Ojeda-Piedra [1,*], Claudia I. García-Betanzos [1], Araceli Ulloa-Saavedra [1], José E. Aguilar-Toalá [2] and María L. Zambrano-Zaragoza [1]

[1] Laboratory of Food Transformation Process and Emerging Technologies, National Autonomous University of Mexico, Cuautitlán Izcalli 54714, Mexico; idalid_gb@unam.mx (C.I.G.-B.); araceli_ulloa@comunidad.unam.mx (A.U.-S.); luz.zambrano@unam.mx (M.L.Z.-Z.)
[2] Department of Food Science, Autonomous Metropolitan University-Lerma, Lerma De Villada 52005, Mexico; j.aguilar@correo.ler.uam.mx
* Correspondence: sergioaop@comunidad.unam.mx

Abstract

Food gels are multiscale materials; their behavior depends not only on composition but also on how their networks are organized from the molecular to the macroscopic scale. This review treats structural scale as a physicochemical design parameter that links formulation, gelation, and food performance. It begins with the building blocks, the molecular bonds that connect them, and the hierarchical architectures of nanogels, microgels, and macrogels. It then examines how material selection, formulation, and processing determine which scale forms. The review compares scale-dependent properties across mass transport, water confinement, mechanical and tribological behavior, and encapsulation, release, stability, and digestion. The comparison reveals a consistent division of roles: macrogels provide shape, firmness, and sustained release; microgels provide soft-particle rheology, lubrication, and interfacial activity; and nanogels best protect and deliver sensitive compounds. This paper discusses food applications alongside key challenges in the field.

Keywords: food gels; structural scale; nanogels; microgels; macrogels; gelation mechanisms; structure–property–function relationships; mass transport; controlled release; food texture

1. Introduction

Food gels are semisolid materials that hold water and lipids inside three-dimensional biopolymer networks. Network organization at multiple scales determines a gel's performance in a product, including texture and stability, water-holding capacity, fat replacement, delivery of bioactive compounds, and compatibility with customized food matrices [1]. Protein and polysaccharide chains form these networks through non-covalent interactions, ionic bridging, and covalent crosslinking. As a result, even modest changes in composition or gelation conditions can alter the network's architecture and behavior [2].

Demand for food products with better nutritional and functional properties has driven interest in natural polymers, including mixed, hybrid, and emulsion gels; fat replacers; matrices for bioactive-compound delivery; and three-dimensional food printing [1,3]. Many recent designs respond to pH, ionic strength, temperature, or gastrointestinal conditions, permitting controlled release and new product formats [4,5]. Research has therefore shifted from describing gel formation to engineering it, enabling control over component distribution, domain size, porosity, and connectivity [4].

Check for updates

Academic Editor: Eduardo M. Costa

Received: 19 October 2026
Revised: 5 November 2026
Accepted: 11 November 2026
Published: 15 November 2026

Copyright: © 2026 by the authors. Licensee MDPI, Basel, Switzerland. This article is an open access article distributed under the terms and conditions of the Creative Commons Attribution (CC BY) license.

Linking formulation, structure, and function in a single account is still difficult. One biopolymer can form structures with very different properties, depending on gel formulation variables such as concentration, molar ratio, and environmental conditions [2]. Processing adds a second layer because it sets the pathways for association, aggregation, and network formation [6]. The resulting structures span several length scales, so their functional properties cannot be read from chemical composition alone; they emerge from organization across the molecular, micro, and macro scales [7].

Recent reviews of food gels usually take material type, gelation mechanism, or a single application as their entry point. Comprehensive reviews organize the field by formation mechanisms, microstructure, functions, and applications [5,6,8]; others focus on one class of building block, such as plant versus animal proteins [9] or gel-forming polysaccharides [10]; on one system, such as emulsion gels as carriers of bioactive compounds or fat replacers [1,7,11] or oleogels [12]; or on one scale, such as protein microgels for texture modulation [3] and microgels and nanogels as encapsulation and delivery vehicles [13–15]. Where multiscale characterization is included, it tends to stay within one system, emulsion gels, for instance, with the emphasis on standardizing production, characterization, and functional evaluation [7], and work that does follow organization from the macroscale to the nanoscale has concentrated on specific classes of biopolymers, proteins above all [16]. What is missing is a model showing how material characteristics and network-forming conditions determine structural scale and how scale reshapes structure–property–function relationships. Earlier frameworks emphasized gelation mechanisms and network design, treating scales as a description of the resulting material. Here, scale is the organizing variable. This review compares the same material, formulation, and processing variables across three scales, focusing on properties rather than systems.

Structural scale is the level of organization at which component distribution and arrangement influence material traits. It goes beyond a gel's external size, from molecular bonds and interchain associations to aggregates, domains, particles, pores, and filaments, up to constant networks that yield macroscopic properties [16]. Nanogels, microgels, and macrogels therefore represent distinct organizational levels, and Sections 5 and 6 develop their functional roles [17].

As shown in Figure 1, this review proposes structural scale as a physicochemical design parameter linking formulation and gelation to food-gel performance. Final structure depends on polymer choice, behavior, and interactions during network formation. Thus, structure–property relationships alone are insufficient; formulation and processing must also link molecular bonding to function, even at comparable compositions, by examining how material selection, physicochemical interactions, and gelation conditions produce nanogels, microgels, or macrogels, and how scale shapes structure–property–function relationships.

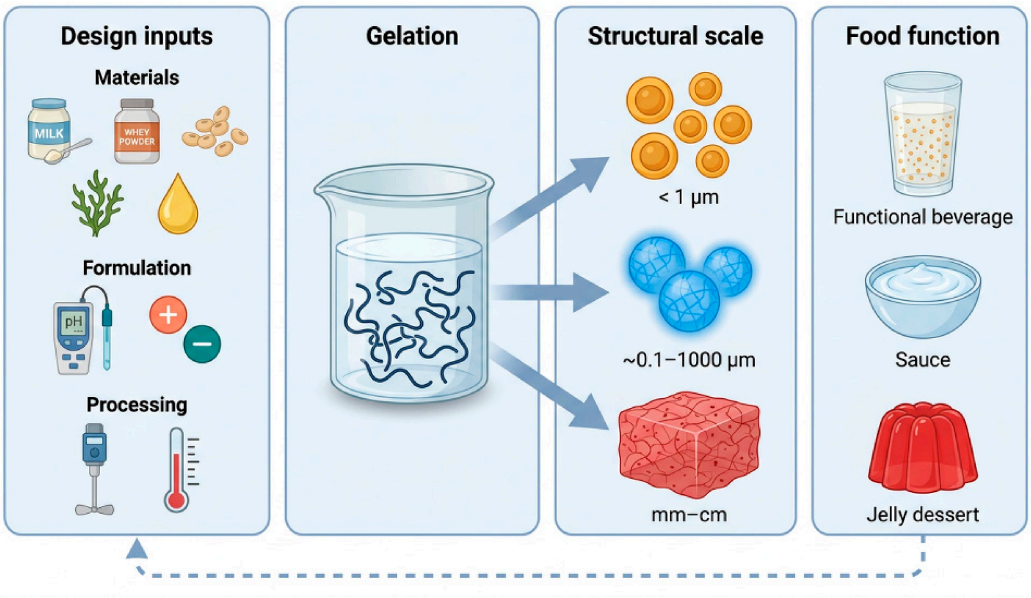


Figure 1. Conceptual framework of this review. Illustration generated with FigureLabs (figurelabs.ai, web-based version) from concepts designed by the authors and subsequently checked and edited by them.

2. Methodology

This narrative review used a structured literature search strategy. Searches were conducted in Web of Science Core Collection, Scopus, and Google Scholar, using combinations of the terms "food gel," "hydrogel," "nanogel," "microgel," "macrogel," "protein gel," "polysaccharide gel," "emulsion gel," "oleogel," "gelation," "structural scale," "microstructure," "rheology," "mass transport," "encapsulation," "controlled release," "digestion," and "food application".

The literature search focused on peer-reviewed publications from 2015 to October 2026. However, earlier studies were included when necessary, particularly when defining widely accepted gelation mechanisms, physicochemical models, or benchmark methodologies. Studies were selected based on their contribution of mechanistic, structural, quantitative, or application-relevant information linking formulation or processing parameters with hydrogel architecture or functionality. Studies lacking sufficient physicochemical relevance to food or food-grade hydrogel systems were excluded from the comparative analysis.

Studies involving gel model systems were included only when they contributed to clarifying mechanisms that have not yet been adequately quantified in food systems. These studies were explicitly identified as model-based evidence derived from experimental systems.

The relevance and quality of the selected studies were evaluated based on methodological clarity, adequacy of structural characterization, consistency between experimental design and conclusions, and their contribution to the structure-property-function conceptual framework considered throughout this review. References were cross-checked across sections to avoid using evidence from a specific application as general proof of a mechanism when the mechanism had not been explicitly demonstrated.

3. Physicochemical Basis of Food Gel Formation

Food gels form when their constituents interact and reorganize into a three-dimensional network [8]. Proteins, polysaccharides, lipids, and their combinations respond to processing through molecular association, aggregation, crosslinking, or crystallization, and the developing network acquires the connectivity, density, and heterogeneity that shape its

macroscopic properties [18]. This section describes the main gel-forming building blocks used in foods, the molecular bonds and gelation pathways that connect them, and the way the resulting structures are organized at different scales.

3.1. Gel-Forming Building Blocks in Food Systems

Food gels combine solid- and liquid-like behavior [8]. They form when components associate, aggregate, crosslink, or crystallize into a continuous network that immobilizes part of the liquid phase, and the strength and stability of that network depend on covalent and non-covalent interactions among its molecules or particles [4]. Depending on the materials and the processing conditions, gels range from homogeneous molecular networks to heterogeneous structures built from aggregated particles, fibrils, or crystalline domains [9]. Proteins, polysaccharides, structured lipids, and their combinations are the most important building blocks [19]. All interconnected structures restrict molecular mobility, but the network is rarely uniform because the building blocks' organization varies with their size, shape, concentration, surface properties, and interactions with other components. Molecular forces generate aggregates, fibrils, crystals, or other supramolecular assemblies that then organize into larger domains and, finally, a macroscopic network [4]. The nature of the building blocks therefore decides both how a gel forms and how its structure develops across length scales.

3.1.1. Molecular Polymers and Particulate Building Blocks

Food gels can develop from molecular polymers or from the assembly of discrete particles [8]. In polymer-based systems, macromolecular chains associate and rearrange until they form a continuous network [8,20] through physical junction zones, intermolecular associations, or covalent crosslinks [8]. Proteins and polysaccharides are the most common molecular building blocks, and their ability to form networks depends on molecular conformation, molecular weight, flexibility, charge, and interactions with water [20]. Particulate gels follow a different pathway: discrete units such as particles, protein aggregates, droplets, or fat crystals associate, aggregate, or pack into a system-spanning network [21], and particle size and shape, deformability, surface characteristics, packing density, and the strength of intergranular interactions then help determine the final structure. Because these units carry their own internal organization, particulate gels are markedly hierarchical [21,22]. Polymeric and particulate gels are nonetheless two ends of a structural continuum rather than separate categories, and many food gels contain both types of structure at once [2,23].

3.1.2. Proteins as Gel-Forming Building Blocks

Proteins are among the most widely used building blocks for food gels because their structure reorganizes in response to temperature, pH, ionic strength, solvent conditions, enzymatic activity, and mechanical treatment, changing how the molecules associate [24,25]. Gelation usually begins with partial unfolding or rearrangement that exposes previously buried groups; these then interact with neighboring molecules, promoting association, aggregation, and network formation [24], and, depending on the protein and conditions, non-covalent and covalent interactions stabilize the network [26].

Globular proteins matter most here: the whey proteins β-lactoglobulin and α-lactalbumin, the egg white protein ovalbumin, the soy globulins glycinin (11S) and β-conglycinin (7S), and pea proteins. Processing unfolds their compact native structures and exposes hydrophobic residues, sulfhydryl groups, and charged regions; the unfolded proteins then associate into soluble aggregates, fibrils, or larger particulate structures before becoming interconnected [27,28]. Whether a fine, homogeneous network or a coarser particulate structure develops depends on the balance between attractive and repulsive interac-

tions, as well as on how fast and how far unfolding and aggregation proceed: the architecture is set by how unfolded proteins associate, not by the extent of denaturation alone [25].

Fibrous proteins offer a different structural basis, because their extended, partially ordered conformations favor extended assemblies. Gelatin, obtained by partial hydrolysis of collagen, illustrates this: on cooling, its chains partially recover ordered conformations and form triple-helical junction zones that act as physical crosslinks, whose extent and distribution influence gel strength, elasticity and thermal reversibility [29]. Because of their high aspect ratio, protein fibrils and other elongated assemblies form interconnected structures at relatively low concentrations, and in these systems fibril organization, rather than concentration alone, controls network connectivity and mechanical function [30].

Protein networks also differ according to protein class and gelation route. Caseins gel primarily through acidification or enzymatic hydrolysis without requiring extensive unfolding [31], whereas gelatin forms thermoreversible networks on cooling through partial helix recovery [29]. Plant proteins have attracted growing interest as plant-based foods expand, and they form networks through different routes: soy proteins aggregate on heating but can also coagulate directly with divalent salts, as in tofu manufacture [32]. Proteins from soy, pea, lentil, chickpea, wheat, rice and other sources gel after thermal treatment, acidification, enzymatic crosslinking or combinations of these [33], although their composition, solubility, aggregation kinetics and sensitivity to pH and ionic strength differ from those of animal proteins and change both the aggregates formed and their organization into the network [9]. Plant proteins also rarely act alone: their interactions with polysaccharides, phenolic compounds, minerals and lipids alter aggregation and create composite structures with distinct microstructural and functional characteristics [34].

Proteins from edible insects, such as crickets and grasshoppers, are an emerging source of gel-forming material that includes muscle, structural, and storage proteins [35]. Their network formation also involves conformational change, aggregation, and intermolecular association, but their techno-functional behavior is more variable than that of purified globular proteins because species, feed, extraction history, residual lipids or chitin, pH, and ionic strength can all alter solubility and aggregation [35,36]. Compared with well-characterized whey, egg, or soy globulins, insect-protein gels therefore tend to show a broader range of mechanical responses and less predictable network homogeneity; however, controlled salt addition, pH adjustment, and thermal processing can increase protein–protein association and strengthen the resulting network [35,36]. Mechanically, this means that insect proteins should not be treated as a single substitute for conventional globular proteins: their gel strength, elasticity, and water retention depend more strongly on fraction composition and processing history, reinforcing the need to relate source-specific molecular characteristics to the final architecture. Because reported gel properties vary widely with species, extraction, and processing, systematic comparisons of the mechanical performance of insect-protein networks with those of conventional globular proteins remain limited, and their behavior when structured at the nano- and microscale is still largely unexplored [35,36].

3.1.3. Polysaccharides as Gel-Forming Building Blocks

Polysaccharides can form a three-dimensional network because their molecular configuration and interactions with water, ions, and neighboring molecules influence chain association during gelation; molecular weight, chain flexibility, branching, and functional groups all play a role [37]. Unlike proteins, polysaccharides typically gel through conformational changes, intermolecular association, helix formation, or physical entanglement into junction zones [6].

Chain architecture determines how those interactions translate into a network. Linear polysaccharides such as agar, carrageenan, and alginate adopt extended conformations that favor interchain interactions and order junction zones [38]. Branching, by contrast, affects chain packing, hydration, and connectivity. Pectin is a good example: its backbone carries neutral sugar side chains that hinder close association of the galacturonic acid sequences, so the balance between smooth and branched regions determines whether ordered junction zones can form [39]. Branching can therefore limit highly ordered structures while increasing the sites available for water interactions, and differences in chain architecture change gel strength, elasticity, and water retention, although these effects are generally reported qualitatively rather than quantitatively [10,40].

Charge provides a second distinction. Neutral polysaccharides, such as many starches and cellulose derivatives, form networks through hydrogen bonding, entanglement, conformational ordering, and sometimes crystalline regions, as in starch, where gelatinization and subsequent reassociation drive gel development and aging [41]. Charged polysaccharides are more sensitive to the ionic environment, so changes in pH and ionic strength alter chain conformation, intermolecular repulsion, and ion-mediated associations [10]. With divalent cations, particularly calcium, alginate chains associate through ion-mediated junctions whose properties depend on polymer concentration, molecular characteristics and calcium availability [42]; pectin behaves more broadly, depending on its degree of esterification and on pH, sugar concentration and ionic conditions, with chains associating through hydrogen bonding, hydrophobic, electrostatic or ion-mediated interactions [39]; and in carrageenan, the number of sulfate groups per repeating unit defines three types: κ-carrageenan, with one sulfate group, gels with potassium and gives firm, brittle networks; ι-carrageenan, with two, gels with calcium and gives soft, elastic networks; and λ-carrageenan, with three and without 3,6-anhydrogalactose, does not gel and is used only as a thickener [10]. Polysaccharides therefore do not act as inert thickeners; they reorganize into networks whose architecture depends on chain conformation, intermolecular interactions, and the surrounding components, making them useful for designing gels with different firmness, elasticity, water retention, and responsiveness to processing.

3.1.4. Structured Lipids and Crystalline Networks

Lipids can also be organized into three-dimensional networks that immobilize liquid oils [12]. These systems, commonly described as oleogels or structured oils, modify the physical properties of oils while keeping a high proportion of liquid lipid [12], which is relevant to foods with modified lipid profiles and to replacing or reducing conventional solid fats [43]. Unlike polymeric gels, lipid-based gels form when crystallizable lipids organize into a continuous network [12]: as temperature falls, crystals nucleate and grow until their surfaces contact neighboring crystals, and van der Waals forces and other intermolecular interactions build an interconnected scaffold that physically immobilizes the liquid oil [12]. The material can therefore behave as a solid even though much of the lipid remains liquid.

The features of these crystalline networks depend not only on the number of solid forms but also on how crystals develop and interact during crystallization [44,45]. Crystal size, morphology, polymorphic form, solid fat content, and crystallization kinetics influence network connectivity and strength; well-distributed, strongly interconnected crystals give more compact, mechanically coherent networks, whereas larger crystals or poorly connected structures give weaker, more heterogeneous materials [46]. Crystallization is thus a structural process that progressively builds a physical scaffold within the oil phase, not a simple liquid-to-solid transition [45,47]. Liquid oils can also be structured with low-molecular-weight gelators and other agents, including waxes, monoglycerides and fatty acids, which self-assemble through non-covalent interactions into crystalline, fibrillar or

supramolecular structures that immobilize the oil [12]. In some systems, this happens across several levels, as molecular association produces small aggregates or fibrils that organize into larger crystalline domains and finally into a continuous network [46]. Oleogels thus show how molecular self-assembly and crystallization translate into higher-order architectures and macroscopic functionality, extending food gelation beyond protein- and polysaccharide-based systems [12].

Table 1 compares four materials: proteins depend on unfolding or charge loss near their isoelectric point; charged polysaccharides respond to ionic conditions and pH near their carboxyl or sulfate groups' pKa; agar and starch gel through cooling or gelatinization; and structured lipid gel through crystallization. These contrasts help predict sensitivity to pH, salts, and temperature before formulation.

Table 1. Characteristics of the main gel-forming building blocks used in food systems.

Building Block	Typical Molecular Weight	Key Structural Feature	pI or pKa	Main Gelation Trigger	Character of the Gel	References
β-Lactoglobulin and whey proteins	~18 kDa (monomer)	Compact globular fold with buried sulfhydryl groups	pI ≈ 5.2	Heating above ~70 °C	Fine-stranded and transparent far from pI; particulate and opaque near pI	[25,28,48]
Caseins	~20–25 kDa (individual caseins, assembled in micelles)	Open, poorly folded chains within colloidal micelles	pI ≈ 4.6	Acidification to ~pH 4.6 or enzymatic hydrolysis	Particulate, weak, prone to syneresis	[31]
Gelatin	~50–200 kDa	Partial recovery of collagen triple helices	pI ≈ 5–9 depending on extraction	Cooling below ~30–35 °C	Transparent, thermoreversible, melts near body temperature	[29]
Egg white proteins (ovalbumin)	~45 kDa	Globular fold, heat-labile	pI ≈ 4.6	Heating above ~70–80 °C	Irreversible; transparent or opaque depending on pH and ionic strength	[26]
Soy proteins (7S and 11S)	~150–200 kDa (7S); ~350 kDa (11S)	Multi-subunit globular assemblies	pI ≈ 4.5–4.8	Heating; divalent salts; acidification	Particulate; 11S forms larger aggregates than 7S	[49]
Pea proteins	~150–400 kDa	Vicilin and legumin fractions	pI ≈ 4.5	Heating; acidification	Coarser and weaker networks than whey proteins	[9,33]
Wheat gluten	Glutenin polymers up to MDa	Disulfide-linked polymeric network	pI ≈ 6.5–7 (gliadins and glutenins)	Hydration and mechanical work; heating	Viscoelastic, extensible	[33]
Alginate	~30–400 kDa	Blocks of guluronic (G) and mannuronic (M) acid	pKa 3.65 (G) and 3.38 (M)	Ca^{2+} binding to G-blocks; pH below ~3	High-G: firm and brittle; high-M: weaker and more elastic; thermostable	[42,50]

Table 1. *Cont.*

Building Block	Typical Molecular Weight	Key Structural Feature	pI or pKa	Main Gelation Trigger	Character of the Gel	References
High-methoxyl pectin	~50–150 kDa	Degree of esterification above 50%	pKa ≈ 3.5	pH below ~3.5 with high soluble solids	Elastic, thermally irreversible	[39,50]
Low-methoxyl pectin	~50–150 kDa	Degree of esterification below 50%	pKa ≈ 3.5	Ca^{2+}, over a wide pH range and low sugar content	Firmer and more brittle; calcium-dependent	[39,50]
κ-Carrageenan	~200–800 kDa	One sulfate group per disaccharide	pKa ≈ 2 (sulfate)	K^+ on cooling	Firm, brittle, prone to syneresis	[10,26]
ι-Carrageenan	~200–800 kDa	Two sulfate groups per disaccharide	pKa ≈ 2 (sulfate)	Ca^{2+} on cooling	Soft, elastic, freeze–thaw stable	[10,26]
λ-Carrageenan	~200–800 kDa	Three sulfate groups; no 3,6-anhydrogalactose	pKa ≈ 2 (sulfate)	Does not gel	Thickener only	[10]
Agar and agarose	~100–150 kDa	Neutral double helices that aggregate	n/a (non-ionic)	Cooling, with marked thermal hysteresis (setting ~35–40 °C; melting ~85 °C)	Firm, brittle, thermoreversible	[51,52]
High-acyl gellan	~200–500 kDa	Acyl substituents that hinder helix aggregation	pKa ≈ 3.5	Cooling with mono- or divalent cations	Soft and elastic	[53]
Low-acyl gellan	~200–500 kDa	Deacylated helices that aggregate extensively	pKa ≈ 3.5	Cooling with mono- or divalent cations	Firm and brittle	[53]
Starch	Amylose ~10^2–10^3 kDa; amylopectin ~10^4–10^5 kDa	Linear and branched glucans in semicrystalline granules	n/a (non-ionic)	Gelatinization at ~55–75 °C followed by retrogradation	Opaque, time-dependent, prone to syneresis	[41]
Methylcellulose	~50–500 kDa	Methyl substituents creating hydrophobic zones	n/a (non-ionic)	Heating above ~50 °C	Thermoreversible on heating; melts on cooling	[54]
Chitosan	~50–500 kDa	Protonatable amino groups	pKa ≈ 6.5	Ionic crosslinking (e.g., tripolyphosphate); pH increase	Requires a minimum chain length for stable gelation	[55,56]

Table 1. *Cont.*

Building Block	Typical Molecular Weight	Key Structural Feature	pI or pKa	Main Gelation Trigger	Character of the Gel	References
Waxes, monoglycerides, and fatty acids	0.3–1 kDa	Crystallizable amphiphiles and low-molecular-weight gelators	n/a for waxes and monoglycerides; fatty acids pKa ≈ 4.8 (carboxyl group)	Cooling below the crystallization temperature	Crystalline network that immobilizes liquid oil; behavior set by solid fat content and polymorphic form	[12,45]

3.2. Molecular Interactions and Gelation Pathways

Building blocks form a gel only when they establish numerous junctions that are persistent and spatially distributed enough to span the system [6]. The chemical nature, strength, and lifetime of those junctions determine whether the network is reversible, how it responds to temperature, pH, and ions, and at which length scale heterogeneity emerges [57]. Several forces usually act at once or in sequence, and their relative contribution shifts as the system moves from dispersed molecules to aggregates and then to a continuous network [6]. Most food gels are held together mainly by non-covalent interactions and are largely reversible, whereas covalent bonds such as disulfide bonds in some protein gels produce more permanent junctions; many gels combine both, making their architecture highly sensitive to formulation and processing [4].

3.2.1. Non-Covalent Interactions

Hydrogen bonds are individually weak but become structurally decisive when many act cooperatively along neighboring chain segments, as in the ordered junction zones of gelatin, carrageenan, agar, and other helix-forming biopolymers, where a coil-to-helix transition is followed by helix association [26,29]. Because hydrogen bonds weaken on heating, gels dominated by them are commonly thermoreversible, and the need to form or break several consecutive bonds explains the thermal hysteresis between setting and melting [58]. Hydrogen bonding with water also governs chain hydration and therefore how the solvent immobilizes the network [59]. Hydrophobic interactions arise mainly from the entropic gain of releasing structured water when nonpolar groups associate, and unlike hydrogen bonds, they strengthen with temperature over the range relevant to food processing [60]. This is why heating promotes the aggregation of globular proteins once unfolding exposes their nonpolar residues [25] and why methylcellulose, whose methyl substituents create hydrophobic zones, gels on heating rather than cooling [54]. Hydrophobic association also drives the self-assembly of amphiphilic proteins and hydrophobically modified polysaccharides into compact domains, a mechanism used to produce nanogels.

Electrostatic interactions can be repulsive or attractive, which makes them one of the most effective tools for controlling gel architecture. Repulsion between like-charged chains or particles slows aggregation and favors extension and swelling. In contrast, attraction between oppositely charged biopolymers, such as proteins below their isoelectric point and anionic polysaccharides, can drive complexation, coacervation, and associative network formation [61]. Their magnitude depends on pH relative to the isoelectric point, the pKa of ionizable groups, and ionic strength [62]. Salts screen electrostatic interactions over the Debye length, approximately $0.304/\sqrt{I}$ nm for a monovalent electrolyte at 25 °C (I in mol L^{-1}): about 3 nm at 10 mM and less than 1 nm at physiological ionic strength [63]. Small changes in salt concentration can therefore switch a system from a repulsion- to an

attraction-dominated regime, which explains the strong sensitivity of particle size to pH and ionic strength. Van der Waals forces are ubiquitous, short-ranged, and individually weak but become significant when surfaces come into close contact [26]; they contribute mainly to the cohesion of particulate networks, protein aggregates, aggregated droplets, and fat crystal networks, where large contact areas multiply their effect [64].

The balance between these forces decides both whether a gel forms and how its structure develops. In heat-set whey proteins, strong electrostatic repulsion far from the isoelectric point and at low ionic strength favors secondary aggregation of thin, flexible strands into transparent, fine-stranded networks. In contrast, near the isoelectric point, with divalent ions or high ionic strength, reduced repulsion leads to dense spherical particles or to microphase separation of strands into particles that associate randomly into opaque particulate gels [48]. The relative magnitude of attractive and repulsive interactions thus sets the typical length scale of a food gel.

3.2.2. Ionic Bridging, Covalent Crosslinking, and Physical Junction Zones

Multivalent ions bridge negatively charged chains, generating junctions whose density depends on ion availability. Calcium binding to guluronate-rich blocks of alginate produces ordered junction zones described by the egg-box model, and low-methoxyl pectin gels through a related calcium-mediated mechanism, although its egg-box dimers differ in formation and structure [50]. Carrageenan and gellan gum gel on cooling in the presence of salts through a coil-to-helix transition followed by helix aggregation, and in gellan the type and concentration of cations determine whether weak or self-supporting gels are obtained [26,53]. In proteins, calcium and magnesium salts coagulate soy proteins during tofu manufacture [32], and in cold-set gelation, preformed heat-denatured whey protein aggregates connect when salts are added or when acidification occurs at ambient temperature [28]. Because chelating agents, competing ions, or pH changes can displace ion-mediated junctions, they offer a route to ecologically responsive gels.

Covalent crosslinks produce more permanent junctions. Disulfide bonds reinforce many protein gels after heat-induced unfolding exposes free sulfhydryl groups [26,65]. Enzymatic crosslinking is milder and more selective: microbial transglutaminase forms ε-(γ-glutamyl) lysine bonds between protein chains and is widely used in dairy, meat, and plant-protein systems [66], whereas laccase and peroxidase crosslink the ferulic acid residues of sugar beet pectin into thermo-irreversible gels [67]. Maillard-type protein–polysaccharide conjugation expands the covalent strategies available [61]. Covalent crosslinking density largely determines mesh size, swelling capacity, and resistance to dissolution [68], parameters that in turn influence transport, mechanics, and digestion.

Physical junction zones are extended zones rather than point-like crosslinks, in which segments of neighboring chains adopt an ordered arrangement: partially renatured gelatin triple helices, carrageenan and agar helix aggregates, and ordered regions formed during starch retrogradation [29]. Their length and tendency to associate laterally into bundles are structurally important: limited association gives fine, relatively transparent networks, whereas extensive bundling generates thicker strands, larger pores, turbidity and, in some cases, syneresis [53]. The crystalline networks of structured lipids are an extreme case, where junctions are contact points between solid crystals [69].

3.2.3. Gelation Triggers as Determinants of Network Architecture

Specific gelation triggers activate the interactions above, and the choice of trigger sets the rate and spatial uniformity of junction formation; therefore, gelation mechanisms are more usefully analyzed by their effects on aggregation and network architecture than as independent categories [6]. Thermal gelation follows two opposite routes. In heat-set

systems, typically of globular proteins, heating induces unfolding, aggregation, and network formation, and the heating rate and holding time balance the formation of new aggregates against their incorporation into the network [70]; under conditions such as prolonged heating at low pH, proteins such as β-lactoglobulin can instead assemble into amyloid-like fibrils whose high aspect ratio allows network formation at low concentrations [24]. In cold-set systems, including gelatin and many polysaccharides, cooling promotes a coil-to-helix transition and helix aggregation [71].

The mode of ion delivery modifies structural uniformity in ionic gelation [72]. When alginate is dripped into calcium chloride, gelation proceeds rapidly from the surface inward, and ion diffusion generates structural gradients. In contrast, internal gelation, in which calcium is released gradually from calcium carbonate by slow acidification with glucono-δ-lactone, produces more uniform networks [72]. In acid-induced gelation of milk, acidification reduces the charge of casein micelles and dissolves part of the crosslinking calcium phosphate, so aggregation begins once electrostatic repulsion no longer counterbalances attraction [73]. Enzymatic gelation provides specificity because the enzyme determines which groups react and how quickly junctions accumulate: transglutaminase bond density can be adjusted by enzyme dosage and reaction time [73], and laccase- or peroxidase-catalyzed pectin gelation accelerates with enzyme dosage, substrate concentration, and temperature [74]. Shear-induced gelation changes spatial organization rather than bond type. Under continuous shear, ordering is confined to discrete domains, producing a suspension of gel particles (a fluid gel) rather than a continuous network [75].

In all cases, the trigger mainly sets the rate of junction formation relative to the rate at which chains and aggregates diffuse and rearrange. Slow, uniform junction formation gives structural units time to reorganize and favor fine, homogeneous networks, whereas rapid or local formation arrests the structure in a heterogeneous, coarser or compartmentalized state [76]. Identical compositions can thus yield markedly different architectures, and this kinetic competition links molecular associations to the final gel's structural scale.

3.3. Hierarchical Design Across Structural Scales

Intermolecular interactions and gelation pathways generate structures organized at multiple scales. Chain conformations and junctions extend over a few nanometers; they give rise to strands, aggregates, and clusters tens to hundreds of nanometers in size, which define pores, particles, and domains at the micrometer scale and, eventually, a continuous network that supports stress at the macroscopic level [51]. Figure 2 summarizes the junction types, the levels of organization, and the architectures found at each scale. Every food gel therefore has more than one distinctive length, and structural scale can refer either to the external dimensions of a gel object, such as a particle or block, or to the dominant internal length of its network, such as mesh, cluster or pore size. The following subsections define these scales and describe the internal architecture of nanogels, microgels and macrogels. Panel (a) groups the interactions by their physical role rather than along a single reversibility axis: non-covalent junctions (hydrogen bonds, hydrophobic association, van der Waals contacts, electrostatic attraction, and ionic bridging) are reversible, with lifetimes that depend on chemistry, temperature, pH, and ionic strength; covalent crosslinks are permanent; and electrostatic repulsion is set apart because it does not form a junction but regulates assembly, swelling, and stability. Whether junctions are reversible decides whether a gel can melt, swell, or be redispersed. Panel (b) follows the same material as it is magnified, from a junction zone a few nanometers across to the bulk gel, and panel (c) shows the four internal architectures that recur throughout the review, from the core–shell nanogel to fine-stranded and particulate networks.

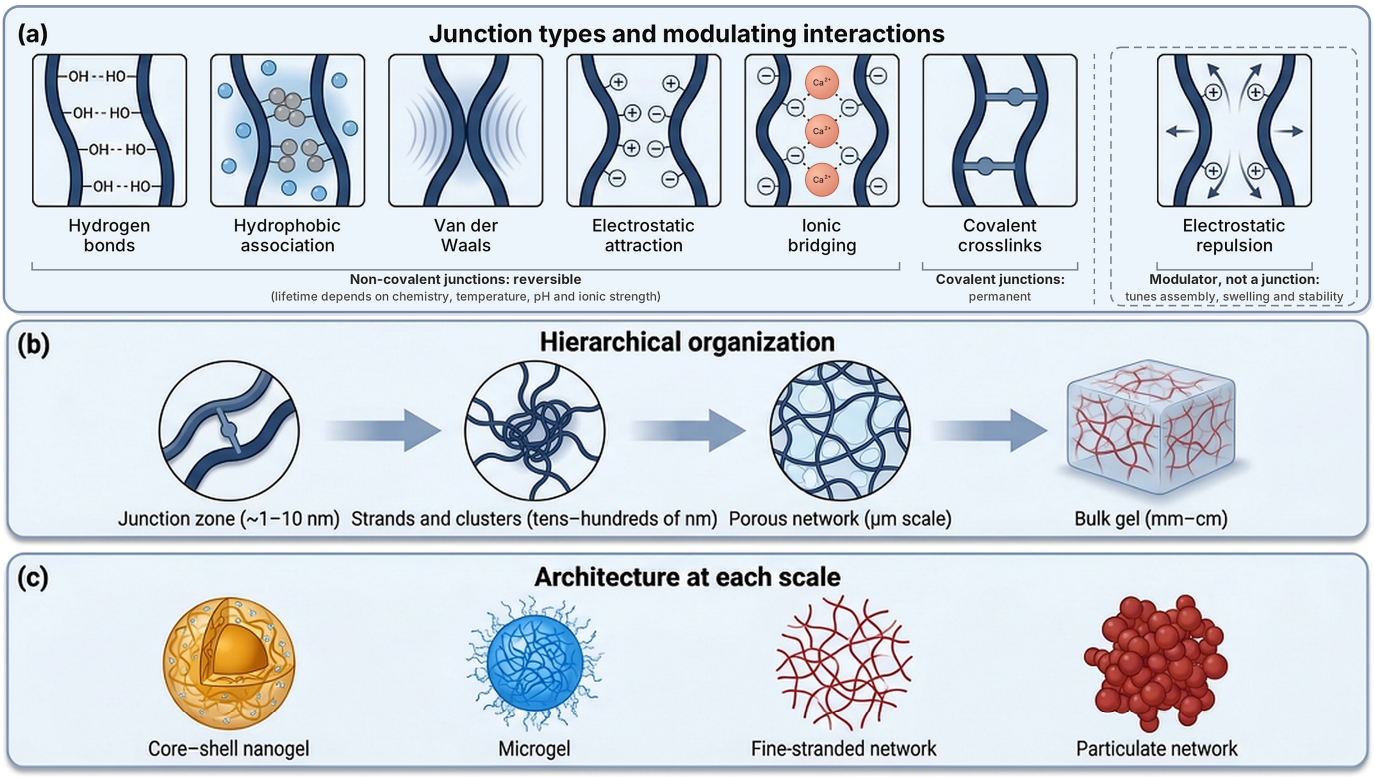


Figure 2. Physicochemical basis of food gel formation: (**a**) interactions grouped by physical role: reversible non-covalent junctions, permanent covalent crosslinks, and electrostatic repulsion as a modulating interaction that does not form a junction; (**b**) hierarchical levels of organization; (**c**) representative architectures at each structural scale. Illustration generated with FigureLabs (figurelabs.ai) from concepts designed by the authors and subsequently checked and edited by them.

3.3.1. Defining Structural Scale

The dimensional boundaries between nanogels, microgels and macrogels remain incompletely standardized [77]. Biopolymer microgels are described as particles about 100 nm to 1000 μm in size, with a crosslinked interior that traps considerable solvent; these particles are sometimes called nanogels, hydrogel beads, or microspheres [13]. Nanogels usually denote the submicron end of this continuum, and both terms often refer to soft, deformable, solvent-penetrable colloids with a gel-like interior [13]. In contrast, macrogels are continuous gels whose dimensions are set by the container, mold, or product [24]. Because these ranges overlap, size alone is not a sufficient criterion, and this review also distinguishes the three categories by their dominant physical behavior: nanogels behave as colloidal carriers governed by their surface and by rapid exchange with the medium; microgels behave as soft, deformable particles that pack, jam, and adsorb on interfaces while retaining a gel-like interior [78,79]; and macrogels behave as space-spanning networks controlled mainly by connectivity and continuity [24]. External and internal scales are not independent: a macrogel may have a few-nanometer mesh, while a microgel may contain nanoscale domains, so always specify the structural length under consideration.

For practical comparison, this review therefore uses an operational framework rather than rigid size cutoffs. Nanogels are defined primarily as colloidal gel particles with characteristic external dimensions in the submicron range (typically < 1 μm) whose behavior is strongly surface- and diffusion-dominated. Microgels are discrete, solvent-swollen gel particles extending from the submicron/micrometer transition to hundreds of micrometers (approximately 0.1–1000 μm in the broader literature), with particle deformability, packing, and interfacial behavior as defining features. Macrogels are continuous sample-spanning

networks whose external dimensions are set by the product or container and are generally millimetric or larger. These ranges intentionally overlap because external particle size, internal mesh size, pore size, and domain size are different structural descriptors; a macrogel can contain a nanoscale mesh, and a microgel can contain nanoscale internal domains. Classification should therefore report both the dimensional descriptor being measured and the dominant physical behavior.

3.3.2. Internal Organization of Nanogels

Nanogels form when network growth is confined to one or a few macromolecules or to small self-assembled domains [80]. Three internal architectures can be distinguished: crosslinked particles in which the polymer is distributed throughout a small, swollen network [81]; core–shell configurations, particularly common in food-grade systems, in which nonpolar segments belonging to amphiphilic polymers form a hydrophobic core surrounded by a hydrated layer, or a protein-rich core is surrounded by polysaccharide chains that provide electrostatic and steric stabilization; and dense spherical particles obtained by controlled heat-induced aggregation of globular proteins such as β-lactoglobulin within narrow pH windows close to the isoelectric point [25]. Because a large fraction of their chains lies at or near the surface, the outer layer largely controls colloidal stability and interactions with food components and biological fluids [82]. Their mesh size often matches the size of encapsulated molecules, making host–guest interactions, rather than simple sieving, decisive for loading and retention [82]. Because diffusion-controlled swelling and solvent exchange scale with the square of the gel dimension, they respond extremely rapidly to environmental change. Their internal organization is difficult to observe directly. Researchers commonly infer this from scattering and super-resolution techniques, which reveal whether the polymer is uniformly distributed or concentrated in a dense core with a looser shell [83].

3.3.3. Internal Organization of Microgels

In microgels, each particle contains a genuine three-dimensional network, while the dispersion is still a fluid or soft solid of discrete units [78]. Their internal organization is frequently inhomogeneous: swollen microgels commonly have a densely crosslinked core surrounded by a fuzzy, loosely crosslinked corona, because crosslinker density decays toward the periphery [83], and biopolymer microgels show analogous gradients that usually originate from the manufacturing route [84]. In top-down approaches, a preformed macrogel is fragmented, so particles tend to be irregular and inherit the internal structure and crosslinking density of the parent gel; in bottom-up approaches, network growth is controlled within emulsion droplets, microfluidic droplets, or sheared domains, giving more regular particles of predefined size and shape [85]. External ionic gelation can create gradients in network density from the surface inward [86], and particles formed under shear, as in fluid gels, are typically elongated or irregular and mechanically entangled with their neighbors, which strongly influences flow behavior [75]. Softness is the defining attribute. Swollen, deformable microgels can be packed beyond the concentration at which rigid particles would jam, and particle elasticity strongly affects their vitrification, jamming, and rheology; the same deformability governs how they spread and pack at oil–water and air–water interfaces and thus their ability to stabilize emulsions and foams [87]. The balance between internal crosslinking density and particle size determines whether a microgel behaves as a hard colloid or a highly deformable object, with direct consequences for rheology, lubrication and fat replacement [3].

3.3.4. Macroscopic Networks

A macrogel forms when junctions and aggregates become connected throughout the sample volume, that is, when connectivity exceeds the percolation point [62]. Two limiting architectures are recognized for protein gels: fine-stranded networks of thin strands that form relatively homogeneous and often transparent gels, and particulate networks of dense aggregates connected into coarser, more heterogeneous and usually opaque structures [25,28], with the balance between attraction and repulsion largely deciding which is obtained. Particulate gels are intrinsically hierarchical, as primary particles associate into clusters that, in turn, connect into the network [21]. Their elasticity depends on the solid volume fraction, but the wide range of experimental dependencies has hindered general scaling principles; recent simulations and rheological analyses explain this via a hidden hierarchical organization of fractal elements, associated with network heterogeneity, that controls the viscoelastic spectrum [21], directly connecting intermediate-scale organization to macroscopic mechanics. These two architectures are readily distinguished experimentally [88]. Scanning electron micrographs of 15% whey protein isolate gels prepared by heat-set gelation revealed fine-stranded aggregates at pH 3 and pH 7. In contrast, gels prepared near the isoelectric point (pH 5) formed larger spherical aggregates. They appeared white and coarse, unlike the smooth, semi-transparent gels obtained at the other two pH values [48]. The same study linked these architectures to functionality: the more elastic gels formed at pH 7 broke into larger particles during simulated oral processing and were digested more slowly in the gastric phase, whereas the brittle gels formed at pH 3 fragmented into smaller particles that were hydrolyzed more rapidly, showing how an architectural difference at the micrometer scale propagates to mechanical attributes and digestion [48].

3.3.5. Mixed, Filled, and Composite Gels

In multicomponent gels, architecture depends on how the components are distributed [24,61]. Segregative interactions yield phase-separated gels with domains enriched in each biopolymer, appearing as dispersed inclusions in a continuous phase or as bicontinuous structures, whose morphology depends on the competition between phase separation and gelation rates; associative interactions yield coupled networks with junctions formed by both biopolymers [26]; and in interpenetrating networks, each component forms its own continuous network within the other, a strategy used to improve mechanical performance [24]. Emulsion gels extend the concept to lipid droplets: in emulsion-filled gels, droplets are embedded in a continuous matrix, whereas in emulsion particulate gels, aggregated droplets are the structural units of the network [89,90]. Droplets bound to the network act as active fillers that generally reinforce the gel, whereas non-interacting droplets act as inactive fillers that tend to weaken it [91]. Bigels combine a hydrogel and an oleogel, and the phase ratio adjusts their mechanical traits and capacity to carry hydrophilic and lipophilic compounds [92]. Macrogels can also be built from smaller gels: hydrogel microparticles packed into granular hydrogels or embedded in bulk hydrogel yield materials whose properties depend on both the particles and their connections [85]. These systems suggest that nano-, micro-, and macroscales can be combined within a single food gel.

The architecture of a food gel thus depends on three linked factors: the nature of the building blocks, the type and kinetics of the interactions connecting them, and the level at which network growth is confined or allowed to percolate [4]. A single protein or polysaccharide can form nanogels, microgels, or macrogels, and within each scale it can produce fine or coarse, homogeneous or heterogeneous structures. The next section analyzes how material selection, formulation, and processing can control this structural scale.

4. Physicochemical Control of Structural Scale

The structural scale of food gel is not a fixed property of the gelling material. It results from how material selection, formulation, and processing govern network growth, that is, from the competition among molecular diffusion, aggregation, phase separation, crosslinking, and kinetic arrest [4,24]. Each group of variables is considered separately below, starting with the material itself. Systematic studies on size control in food-grade gels remain scarce, so we illustrate some mechanisms using well-characterized synthetic systems, such as poly(pNIPAm) microgels, but only where the underlying principle also applies to protein- and polysaccharide-based gels [93].

This control operates over a broad range. Figure 3 plots the sizes reported in experimental studies of food and food-grade gels on a single logarithmic axis, spanning roughly six orders of magnitude—from ovalbumin gel nanoparticles measuring 40–60 nm to whey protein gel pieces several millimeters long. Two systems appear twice. After wet pulverization, amylose–polysaccharide gels shrink from tens of micrometers to a few hundred nanometers, while α-lactalbumin–chitosan particles grow from about 100 nm to aggregates more than 400 nm in radius when high-molecular-weight chitosan is used. These examples show that the same composition can result in very different scales.

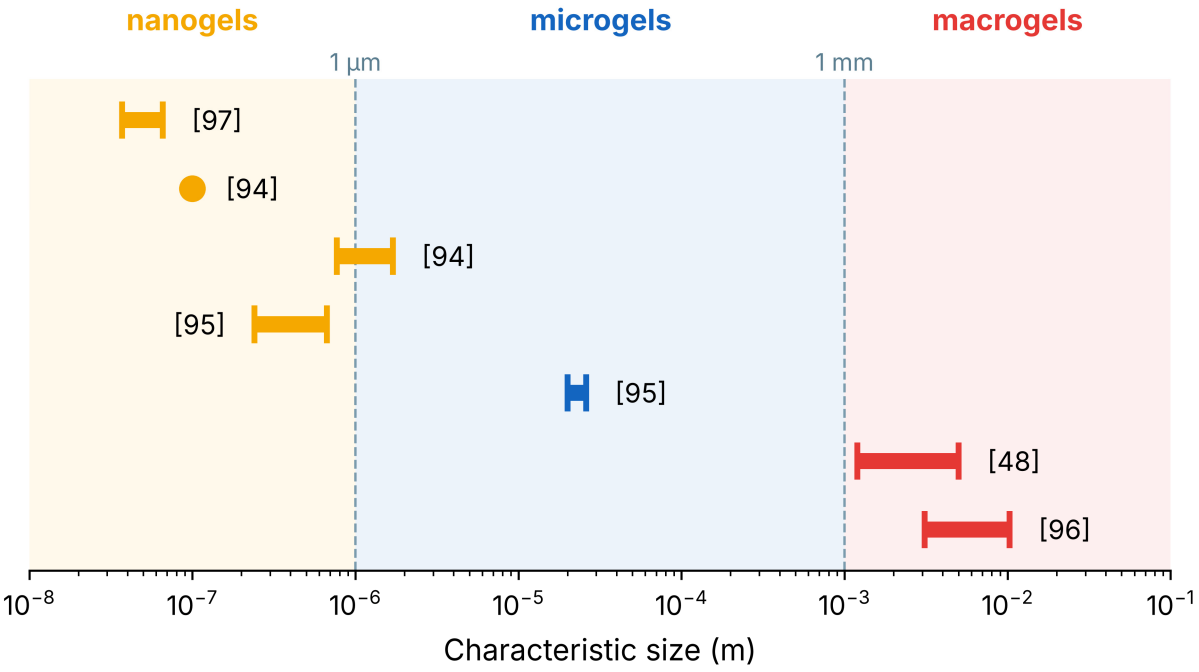


Figure 3. Structural scales reported for food and food-grade gels [48,94–97], plotted on a logarithmic size axis; colors indicate the nano-, micro-, and macroscale, and dashed lines mark the 1 µm and 1 mm boundaries. From top to bottom: ovalbumin gel nanoparticles measured by TEM [97]; α-lactalbumin–chitosan nanogels [94]; α-lactalbumin–chitosan–PEG [94]; amylose–polysaccharide gels after wet pulverization at 200 MPa [95]; the same gels before pulverization [95]; minced whey protein gels [48]; and whey protein gel pieces (cubes and spheres) [96]. Original figure generated by the authors from data reported in [48,94–97] plotted in Python 3.13 (Matplotlib 3.11).

4.1. Influence of Material Selection

Gels are three-dimensional polymeric networks with high water content, formed when hydrophilic chains are crosslinked in water through physical, electrostatic, or covalent interactions [98]. Main gel-forming polysaccharides include alginate, chitosan, hyaluronic acid, dextran, cellulose, agarose, and starch, and the most-studied proteins include collagen, gelatin, silk fibroin, caseins, albumins, and other polypeptides [99]. Because size boundaries

between the three scales are not standardized, the subsections below focus on the variables that shift a system toward one scale or another.

Polymer Nature, Protein-to-Polysaccharide Ratio, Molecular Weight, Flexibility, Branching, Charge, and Hydrophobicity

Polymer type matters because each macromolecule class forms networks differently. Polysaccharides have numerous hydroxyl, amino, and carboxyl groups that can participate in ionic crosslinking, hydrogen bonding, and covalent interactions, making them suitable for hydrogels and self-assembled nanogels [98]. Proteins combine polar groups, charged regions, nonpolar side chains, and peptide conformations, enabling both noncovalent association and chemical crosslinking. Polymer type alone does not determine particle size; rather, it provides the functional groups, chain architectures, and assembly pathways that favor formation of a macrogel, microparticle, or nanoparticle. Researchers can produce microgels from any gelling polysaccharide. Hyaluronic acid, alginate, chitosan, and heparin are widely used because they allow network architecture and pore size to be tuned across a broad range [78]. By contrast, polysaccharide nanogels generally require physical or chemical crosslinking to form submicron networks [100]. A comparison of agar, curdlan, and gellan gum microgels prepared using bottom-up and top-down routes showed that functionality depended on particle size rather than polysaccharide identity. Agar and curdlan microgels gave polysaccharides that are not surface-active in solution the ability to emulsify, whereas gellan gum microgels did not; emulsions stabilized with curdlan also resisted centrifugation better than those stabilized with agar [101]. In amylose gels containing ionic polysaccharides such as 4-O-methyl-D-glucurono-D-xylan, alginate, or xanthan, gelation under shear followed by wet pulverization at 200 MPa reduced particle size from the micrometer to the submicrometer range. The added polysaccharides increased the particles' surface charge and improved dispersion of the amylose–polysaccharide nanofibrils, which otherwise were partly aggregated [95].

In proteins, type influences behavior mainly through unfolding, charge development, and aggregation, although the relationships between molecular properties and aggregation behavior are complex and not always easy to establish [102]. Globular proteins are well suited to nanogel formation because controlled heating reorganizes their structure. Under favorable pH, protein concentration, and divalent ion levels, β-lactoglobulin and whey protein isolate form spherical particles measuring 70–200 nm. Stable nanogels form when the net charge remains within approximately 3–5 charges per molecule; outside that range, fibrils or larger aggregates predominate [65]. Mineral composition and the relative proportions of proteins also affect microgel yield and size [103]. In mixed systems, particle size depends more on interactions between proteins and polysaccharides during assembly than on either polymer alone [104]. Electrostatic attraction, hydrogen bonding between carboxyl and amino groups, and hydrophobic association following partial denaturation drive chains to form compact particles that minimize free energy [105]. In maleic anhydride-functionalized chitosan–bovine serum albumin nanogels, size decreased as pH rose to approximately 4.7, near the isoelectric point of BSA and above the polysaccharide's pKa. It then increased at higher pH as both macromolecules deprotonated [104]. Core–shell assembly commonly produces particles of approximately 100–300 nm, although particles as small as 32–40 nm have been reported. The most highly charged formulation had more polysaccharide chains extending from the protein surface and was larger [106]. Protein–polysaccharide gels therefore respond more sharply to formulation changes than single-polymer gels because they involve more interactions [104,106,107].

The protein-to-polysaccharide ratio governs the balance between internal network formation and aggregation. Near-stoichiometric ratios enable more charged sites to participate,

producing well-defined particles or highly connected networks. By contrast, imbalanced ratios leave free chains or excess charge, resulting in incomplete or heterogeneous structures [108]. In macrogels, protein-rich systems form denser networks with smaller pores, whereas polysaccharide-rich systems form more hydrated, porous networks [2]. Charged polysaccharides can also screen protein surface charge; too little screening keeps particles apart, while too much promotes large-scale aggregation [109]. The ratio also sets the strength of the parent network, since potato protein microgels obtained from precursor gels (100–300 nm) increased in size with protein concentration, showing a direct link between precursor gel strength and particle size [110].

Molecular weight modifies flexibility, intra- and intermolecular interactions, conformation, and solubility, thereby affecting particle nucleation, growth, and interconnection [111]. Longer chains increase overlap and viscosity much as a higher polymer concentration does [112], whereas short chains tend to stay separate, associate intramolecularly, or form limited clusters, and a minimum chain length may be required—chitosan–tripolyphosphate gels, for instance, need a viscosity-average degree of polymerization above 152 [55]. In model core–shell nanogels, increasing the shell-forming polyamine's molecular weight from 0.6 to 10 kDa more than tripled the polymer immobilized at the surface and increased particle size [113]. High-molecular-weight soy protein isolate forms stronger cohesive networks that fragment into larger, compact particles, whereas partially hydrolyzed proteins form weaker networks that break into smaller ones [114]; the 11S soy fraction forms larger aggregates than the 7S fraction, which can occupy the spaces between aggregates and modulate viscoelasticity [49]. Molecular weight alone does not always explain size: acylated rapeseed protein formed nanogels of approximately 170 nm with a hydrophobic core and a hydrophilic shell because acylation altered chain association [115]. In protein–polysaccharide systems, molecular weight is meaningful only together with charge, ratio, pH, ionic strength, and temperature [104,106]: short polymers limit the size of initial complexes, and longer chains establish more bridging interactions [116]. In α-lactalbumin–chitosan nanogels, most formulations stayed near 100 nm, but mixtures containing 113 kDa chitosan–PEG formed precipitating aggregates with hydrodynamic radii above 400 nm at pH above 5 [94], so higher polysaccharide molecular weight can either protect proteins against uncontrolled heat-induced aggregation or promote large, unstable aggregates [94,104].

Flexibility controls how chains move, fold, entangle, and reorganize through two opposing processes: flexible chains can fold and interpenetrate within a particle, giving denser packing and smaller particles, but their mobility also increases collisions. This can favor larger aggregates [117]. Lower crosslinker concentrations generate more flexible networks with more ordered packing in nanogels [118], whereas in swollen microgels longer chains between crosslinks allow more expanded conformations and larger swollen sizes [119]. In proteins, lower flexibility may slow rearrangement, and larger, mechanically stronger microgels have been reported to be less flexible and to diffuse more slowly toward interfaces [110]. Flexibility thus reduces size when rearrangement improves local packing and increases it when it mainly promotes collisions, coalescence, or chain expansion.

Charge density sets repulsion between chains and therefore swelling and stability [120]. More like charges raise counterion osmotic pressure and electrostatic repulsion, expanding the network and the hydrodynamic diameter [121], as when chitosan nanogels swell at low pH through amino group protonation [56]. Charge also controls aggregation: strong association between oppositely charged proteins and polysaccharides can limit heat-induced protein aggregation [94]; in xanthan–blueberry leaf polysaccharide gels, higher charge density raised the absolute zeta potential and gave smaller particles until neutralization reversed the trend [122]; and in protein–polysaccharide nanogels, a more highly charged shell can increase hydrodynamic size [106]. Higher charge density therefore tends to

increase size through swelling and chain extension, whereas a lower effective charge reduces swelling but raises the risk of aggregation or ionic crosslinking [123].

Branching and degree of substitution shift the balance between compact assembly and swelling [124]. Nanogels of approximately 100–400 nm have been reported depending on substitution [125]; in hydrophobically modified methylcellulose nanogels, the degree of hydrophobization decided whether molecular weight mattered, with longer chains increasing swelling capacity and particle size in water at a low degree of modification and no significant effect at a high one [126]. Higher substitution does not always reduce size, since short, distributed substituents may promote compaction, whereas fewer but longer side groups may generate larger assemblies. Modified soy protein–dextran nanogels formed core–shell particles of 57–66 nm, compared with about 138 nm for the unmodified system [106]. Tight chain packing favors smaller particles; extended chains or strong steric constraints favor larger ones.

Hydrophobicity governs chain affinity for water and thus affects both early assembly and the solvent retained in the final network. In hydrophobically modified polymers, nanogel size increased with alkyl chain length and grafting degree, consistent with stronger hydrophobic attraction during self-assembly [118], and more hydrophobic proteins likewise form larger particles [117]. Once a crosslinked particle has formed, lower polymer–water affinity has the opposite effect: simulations show that a higher Flory interaction parameter promotes water expulsion and reduces microgel size [119], and in soy protein–dextran nanogels, hydrophobic groups exposed by denaturation or hydrolysis promoted self-assembly and more compact internal structures [106]. The net effect therefore depends on the stage: hydrophobicity enlarges particles during assembly but shrinks them once the network forms, and size depends mainly on swelling.

4.2. Influence of Formulation

pH, Polymer Concentration, Ionic Strength, and Crosslinking Agent

In pH-responsive gels, size usually increases when ionizable groups become charged, because repulsion expands the network and increases water uptake. Hyaluronic acid nanogels grew with pH, particularly above the pK_a of their carboxyl groups (~5) [127], as reported for carboxyl-containing synthetic nanogels and microgels [128]. The opposite occurs when positive charge is lost as pH rises: amine-containing nanogels shrink between pH 8.5 and 10 [128], and chitosan–genipin microgels deswell at pH 8, more so when less crosslinked [129]. The effect is strongest near the pK_a, and protonation of carboxyl groups below their pK_a also reduces repulsion and promotes aggregation, as in carboxyl-functionalized microgels [113]. pH thus acts through two linked mechanisms, one on network charge and swelling and one on interactions between particles; depending on which dominates, a system may swell, contract, grow, or aggregate.

The most common effect of salt is deswelling because counterions screen repulsion between charged chains [130]; in anionic hollow microgels, raising ionic strength from 0.1 to 50 mM reduced the hydrodynamic radius from about 380 to 220 nm [130], with similar reductions in other ionic microgels [131] and in chitosan–genipin microgels in 150 mM NaCl [129]. In some cationic nanogels, crosslinker concentration becomes dominant at sufficiently high salt [128], and salts can lower the volume phase transition temperature at which chains lose affinity for water, expel solvent, and collapse [132]. The behavior is not universal, because screening can also enhance particle association and growth during assembly; salt therefore affects both the swelling of formed gels and the assembly of new ones [133].

Higher polymer concentration commonly produces larger particles, although component proportion and chemistry also act through viscosity, hydrophobic association, charge

balance, and interchain crosslinking [118,132,134]. Doubling monomer concentration increased model acrylamide-based nanogels from 5–10 to 16–26 nm [135]; higher polymer concentrations produced larger hybrid nanogels [136]; and reducing chitosan concentration from 0.5 to 0.35% w/w decreased particle size from 157 to 92 nm through lower viscosity and easier droplet breakup [134]. Two mechanisms explain these trends: higher viscosity yields larger precursor droplets during mixing or emulsification [134], and stronger intermolecular interactions increase interchain crosslinking [135,136]. Exceptions arise when concentration changes also change crosslinking density, since more crosslinkers can produce more compact and smaller particles [136].

Crosslinking agents modify size both during and after network formation [137]. During synthesis, more crosslinkers can generate more junctions, accelerate gelation, and produce larger nuclei, yielding larger, less polydisperse nanogels [137] and larger chitosan nanogels at higher tripolyphosphate concentrations [138]. In formed networks, higher crosslinking density shortens the distance between junctions and restricts chain mobility, so densely crosslinked gels are smaller when swollen; in pH-responsive nanogels, the volumetric swelling ratio fell from about 740% to 250% as crosslinker content increased [139]. The net effect therefore depends on whether size is measured during formation or in the swollen state [127]. The chemical identity of the crosslinker matters as much as its concentration because rigidity, hydrophobicity, spacer length, and crosslinking efficiency all influence size and swelling [127]. Table 2 quantifies several of the trends described above. Its rows come from individual studies, and the column that labels each system as food or model deserves attention: chitosan–tripolyphosphate gels, hydrophobically modified methylcellulose, and hollow anionic microgels quantify mechanisms clearly, but they are not food-grade, whereas the whey protein, agarose, agar, curdlan, gellan, and amylose systems are. The last rows go one step further by linking structure to lubrication, digestion, and the chemical stability of an encapsulated compound, showing why gel size matters beyond its dimensions.

Table 2. Quantitative findings from studies on gel systems illustrate how material, formulation, and processing variables modify structure and behavior.

System	Type	Variable Studied	Reported Findings	Reference
Heat-set whey protein isolate gels (15%)	Food	pH of gelation (3, 5, 7)	Fine-stranded aggregates at pH 3 and 7 versus larger spherical aggregates at pH 5; after mincing, mean particle diameters of 1.32, 1.29 and 4.62 mm, respectively; gels prepared at pH 7 released less than 20% filterable nitrogen after 30 min of gastric digestion, against ~100% for gels at pH 3 and 5	[48]
Whey protein gels of defined geometry	Food	Particle geometry (cubes of 3.1, 5.2 and 10.3 mm; spheres of 6.5 mm)	Spheres broke down mainly by erosion and cubes by fragmentation followed by erosion; higher pepsin activity in the liquid phase with large cubes, attributed to limited pepsin diffusion into particles of lower specific surface area	[96]
Whey protein emulsion gels	Food	Gel structure (hard versus soft)	Slower disintegration and protein hydrolysis in the hard gel during gastric digestion; bioaccessibility of capsaicinoids related to the extent of lipid digestion	[140]

Table 2. *Cont.*

System	Type	Variable Studied	Reported Findings	Reference
Agarose fluid gels	Food	Polymer concentration (0.5, 1 and 2 wt%)	Storage and loss module increased with concentration; the 1 wt% fluid gel showed the lowest viscosity at low shear and the shortest linear viscoelastic range; particle size and the amount of unordered chains at the particle surface changed with concentration.	[52]
Agar, curdlan and gellan gum microgels	Food	Polysaccharide type and preparation route (bottom-up versus top-down)	Agar and curdlan microgels imparted emulsifying ability to otherwise surface-inactive polysaccharides, whereas gellan gum did not; particle size was decisive for emulsifying ability, and curdlan-stabilized emulsions resisted centrifugation better than agar ones	[101]
Amylose gels with ionic polysaccharides	Food	Wet pulverization after gelation under shear (200 MPa)	Particle size reduced from 20–26 µm to 240–670 nm; the ionic polysaccharides increased surface charge and improved the dispersion of the amylose–polysaccharide nanofibrils	[95]
Plant protein microgels	Food	Conversion of a percolated protein gel into microgels	Boundary friction decreased by about one order of magnitude relative to the native proteins, matching the lubrication performance of an oil-in-water emulsion	[17]
Curcumin-loaded emulsions and nanoemulsions	Food	Oil droplet size	Chemical stability of curcumin during storage decreased as droplet size diminished.	[141]
Chitosan–tripolyphosphate gels	Model	Molecular weight and degree of acetylation	Stable gels required a viscosity-average degree of polymerization above 152; stiffness and rupture strength increased with molecular weight, whereas higher acetylation reduced the shear modulus but increased elasticity.	[55]
Hydrophobically modified methylcellulose nanogels	Model	Backbone molecular weight and degree of hydrophobization	At a low degree of hydrophobization, higher molecular weight increased swelling capacity and particle size in water, whereas no significant effect was observed at a high degree of hydrophobization; nanogels from 30 kDa methylcellulose retained less dexamethasone and released it faster than those from 230 kDa	[126]
Hollow anionic microgels	Model	pH and ionic strength	pH and ionic strength-controlled particle size and its internal cavity; adding salt reduced the fuzziness of the outer surface while increasing that of the internal cavity.	[130]

4.3. Influence of Processing

Particle size is not set by chemistry alone but by the balance between processing forces that deform and fragment droplets or partially gelled regions—shear, mixing, flow—and forces that resist breakup, including viscosity, interfacial tension, and incipient gelation [142]. Processing therefore acts through fragmentation intensity, coalescence probability, and the rate at which the structure becomes rigid enough to prevent further change.

Mixing, Temperature, Pressure, Shear, and Gelation Rate

Higher shear rate or mixing intensity generally decreases size, because stronger hydrodynamic stresses overcome interfacial and cohesive forces; in hydrogel emulsions and microgels, higher mixing speeds and longer treatments reduced average size and narrowed the distribution [143,144]. Shear does not act only through breakup: at low or moderate levels, flow can orient chains, bring nuclei together, and promote local aggregation, and in biopolymer gels formed under shear, particles may nucleate and grow before the same shear field disrupts them [52]. The Mason number often captures this balance: weak shear promotes network rearrangement, while strong shear progressively erodes the structure into dispersed particles [145]. In fluid gels, continuous flow during gelation restricts the growth and interconnection of gelled domains, yielding irregular particles whose dimensions depend on polymer type, gelation mechanism, and shear rate; higher shear generally produces smaller particles and mild shear larger ones, although in some systems size increases with shear up to a critical value and then stabilizes [146]. Mixing also acts indirectly through gelation kinetics: higher mixing rates delayed curing in sheared suspensions and extended the period in which shear could reduce size [142], and in alginate crosslinked with $CaCO_3$, higher shear delayed gelation onset, whereas lower shear allowed rapid particle growth [147]. Insufficient shear can cause poor dispersion, incomplete hydration, or broad distributions, while excessive shear can disrupt the network or reduce particle integrity even as average size decreases [142].

Temperature modifies the rate of structural development and the time available for breakup, coalescence, and relaxation before the structure is fixed, and gel behavior is closely linked to the temperature of network formation [148]. In heat-responsive systems, higher temperatures increase molecular mobility, collision frequency, and hydrophobic association, accelerating aggregation and network development [149]. Fast gelation can limit the growth of small structures generated during fragmentation but can also preserve large aggregates formed early; during thermally induced gelation of polysaccharides under shear, conformational ordering competes with cooling rate and the time scale of shear, so slow gelation lets droplets relax into spherical particles whereas rapid ordering traps larger, anisotropic structures [150]. In emulsion-templated systems, gelatin emulsion gels processed at 35 °C and cooled slowly produced more uniform particles [151], whereas cold-induced gelation of methacrylated gelatin in an ice bath let droplets merge before stabilization, yielding larger microparticles [152]; heating and cooling rates thus shape microstructure during formation [153].

When fabrication involves pressure or flow, size is often set when droplets detach from the liquid stream [154]. Higher continuous-phase flow rates, gas pressures, or drag forces generally produce smaller and more uniform particles, provided gelation is not so fast that it causes clogging or occurs before detachment, since size reflects the balance between the detaching force and the resistance associated with viscosity and interfacial tension [155]. Whey protein microgel beads produced by microfluidic emulsification were more monodisperse than those obtained by batch emulsification, and their size could be tuned through the oil and aqueous flow rates [156]; microfluidic methods generally allow sizes of approximately 5–1000 μm [157]; and in air-assisted coaxial injection, raising air pressure from 40 to 180 kPa reduced alginate microgels from 202 ± 14 to 49 ± 4 μm [158]. Flow rate can also affect polymer distribution and crosslinking density within droplets and hence particle elasticity and swelling [159].

Finally, gelation rate determines whether structures are fixed before or after they can grow [152]. Early ionic crosslinking stabilizes dimensions and yields smaller, more uniform microparticles, whereas slower temperature-dependent gelation allows droplets to merge [152], and more highly crosslinked particles swell less and remain smaller [159].

Rapid gelation does not always produce small particles: in polysaccharides gelled under shear, large anisotropic particles formed when ordering was so fast that gel structures developed before fragmentation, whereas slower crosslinking favored smaller, more spherical particles [150]. Particle size thus depends on the balance between crosslinking and fragmentation rates, and gelation under flow can convert what would otherwise become a continuous gel into dispersed particles [160].

Table 3 gathers the material, formulation, and processing variables in one place, together with the direction in which each one usually moves particle size and the mechanism behind it. The word [104,109] is usually deliberate. Several variables act through competing mechanisms: crosslinker concentration can enlarge particles during synthesis and shrink them once the network has formed, and moderate shear may favor aggregation where strong shear breaks the structure apart. The table is therefore best read as a guide to the first variable worth adjusting, not as a set of fixed rules.

Table 3. Typical effects of material, formulation, and processing variables on the structural scale of gels.

Variable	Typical Effect on Size or Scale	Main Mechanism	Representative Example	References
Polymer type	Determines the assembly route toward nano-, micro-, or macrostructures	Functional groups, chain architecture, and gelation mechanism	Agar and curdlan microgels imparted emulsifying ability to otherwise surface-inactive polysaccharides, whereas gellan gum microgels did not; particle size was decisive	[101,116]
Protein:polysaccharide ratio	Near-stoichiometric ratios give defined particles or connected networks; imbalanced ratios give heterogeneous or aggregated structures.	Participation of charged sites; charge screening	Chitosan–BSA nanogels reached minimum size near pH 4.7	[104,109]
Molecular weight	Usually increases size; a minimum chain length may be needed for gelation	Chain overlap, viscosity, and interchain bridging	α-Lactalbumin with 113 kDa chitosan–PEG formed precipitating aggregates with hydrodynamic radii above 400 nm at pH > 5, against ~100 nm for the other systems; chitosan–tripolyphosphate gels required $DP_v > 152$	[55,94]
Chain flexibility	Decreases size when packing improves; increases it when collisions or swelling dominate	Local rearrangement versus chain collision and expansion	Less crosslinked, more flexible networks reach larger swollen sizes	[117,119]
Charge density	Increases size through swelling; can decrease it by limiting aggregation	Electrostatic repulsion and counterion osmotic pressure	Xanthan–blueberry leaf polysaccharide gels became smaller with charge until neutralization	[56,122]
Substitution and branching	The degree of substitution determines whether molecular weight affects size	Chain packing versus steric hindrance and swelling	In hydrophobically modified methylcellulose nanogels, higher molecular weight increased swelling and size at a low degree of hydrophobization, with no significant effect at a high degree	[106,126]

Table 3. *Cont.*

Variable	Typical Effect on Size or Scale	Main Mechanism	Representative Example	References
Hydrophobicity	Increases size during self-assembly; decreases swollen size in formed networks	Hydrophobic association versus water expulsion	Acylated rapeseed protein formed core–shell nanogels of ~170 nm	[115,119]
pH	Increases size when network groups ionize; promotes aggregation when charge is lost	Network swelling and interparticle interactions	Hyaluronic acid nanogels grew above pK_a; chitosan–genipin microgels deswelled at pH 8	[127,129]
Ionic strength	Usually decreases size by deswelling; may increase it during assembly	Electrostatic screening	Anionic hollow microgels shrank from ~380 to ~220 nm (0.1–50 mM)	[130,133]
Polymer concentration	Usually increases size, except when crosslinking density also changes	Viscosity, droplet size, and interchain crosslinking	Chitosan particles decreased from 157 to 92 nm (0.5–0.35%)	[134,136]
Crosslinker concentration	Increases size during synthesis; decreases swollen size after formation	Faster nucleation versus restricted swelling	Larger chitosan–TPP nanogels at higher TPP content	[138,139]
Shear and mixing	Strong shear decreases size; weak shear may promote growth	Fragmentation versus collision and aggregation	Smaller fluid gel particles at higher shear	[52,161]
Temperature and cooling rate	Slow ordering gives uniform, spherical particles; rapid ordering or slow stabilization gives larger ones.	Ordering kinetics versus droplet relaxation and merging	More uniform gelatin emulsion gels after slow cooling	[150,151]
Flow rate and pressure	Higher flow rate or gas pressure decreases size and polydispersity	Droplet detachment from the liquid stream	Alginate microgels decreased from ~202 to ~49 µm (40–180 kPa)	[156,158]
Gelation rate	Early crosslinking fixes small particles; very rapid ordering can produce large fragments	Crosslinking rate versus fragmentation rate	Smaller microparticles with early ionic crosslinking	[152]

BSA: bovine serum albumin; DPv: viscosity-average degree of polymerization; TPP: tripolyphosphate.

4.4. Formation of Nano-, Micro-, and Macrogels

Across these scales, polymer nature, the hydrophilic–hydrophobic balance, the type and extent of crosslinking, solvent conditions, and stimuli such as pH, temperature, mechanical stress, and ionic strength govern the final structure. Nanogel formation is favored when crosslinking occurs within a single chain or small aggregate before neighboring chains connect over longer distances [162] and when the space for network growth is restricted, as in the self-assembly of amphiphilic polymers, where hydrophobic segments associate and hydrophilic segments face the water, generating small domains that can be stabilized by crosslinking [163]. Short residence times and high flow rates generate numerous nuclei while limiting their growth [164], and low-viscosity dispersed phases are more easily broken into small particles. However, excessive stress increases collisions and coalescence [143]. Premature precipitation or aggregation favors growth beyond the nanoscale, so ionic conditions must allow a nanoscale network to develop before macro-

scopic phase separation begins [123], and sufficient crosslinking is needed because weakly crosslinked particles may swell until they lose their morphology [165]. Microgel formation is favored when gelation is restricted to discrete droplets, nuclei, or polymer-rich domains that grow beyond the nanoscale without merging into a continuous gel [166,167]. Interchain association must be strong enough to produce particles from approximately 100 nm to hundreds of micrometers. Yet, long-range connectivity must remain below the macrogel threshold, generally associated with an intermediate crosslinking density that provides mechanical stability while permitting swelling [15,93]. Too little crosslinking produces weak particles; excessive interparticle connectivity shifts the system toward aggregation or continuous gelation [93,168]. Microgels therefore form when pH, temperature, or salt conditions generate interactions strong enough to build a network within each particle without extensive connectivity between particles [15,93]. Macrogel formation occurs when locally crosslinked domains connect beyond the percolation threshold into a continuous, system-spanning network, favored by intermolecular rather than intramolecular or localized crosslinking and by the absence of spatial constraints that confine gelation to droplets or compartments [169]. Macrogels can also be assembled from microgels acting as building blocks, as in supramolecular macrogels built from supramolecular microgels [170].

Figure 4 brings these conditions together. The bar at the top runs from confined to percolating growth, and the three rows that branch from the same biopolymer solution are alternatives, not stages: self-assembly or rapid flow through narrow channels for nanogels; emulsion templating, microfluidic droplets, or shear during gelation for microgels; and gelation without spatial confinement for macrogels. The balance at the bottom carries the central message, since the final scale depends on whether junctions form faster than the structure fragments, coalesces, or relaxes.

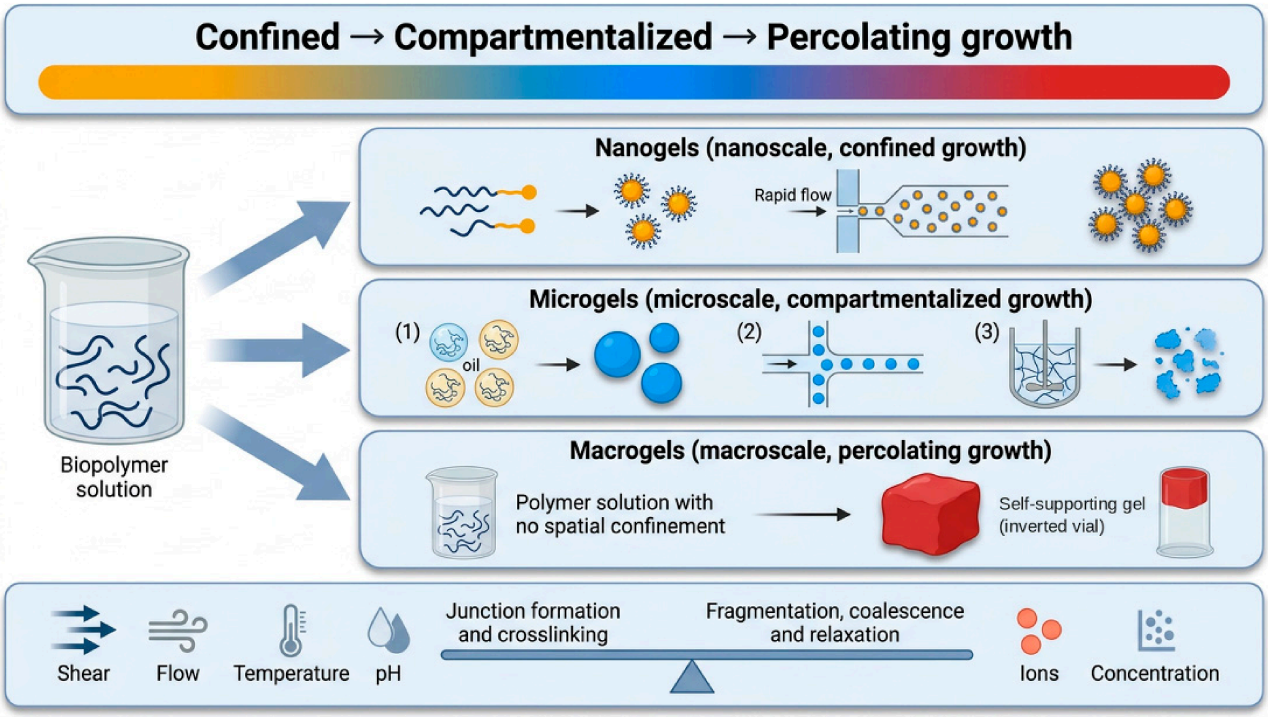


Figure 4. Control of structural scale: fabrication routes and conditions that favor the formation of nanogels, microgels, and macrogels. Numbers in the microgel panel indicate the main fabrication routes: (1) emulsion templating, in which biopolymer droplets dispersed in an oil phase act as gelation compartments; (2) microfluidic droplet generation; and (3) mechanical fragmentation of a bulk gel under shear (top-down approach). Illustration generated with FigureLabs (figurelabs.ai) from concepts designed by the authors and subsequently checked and edited by them.

5. Scale-Dependent Physicochemical Properties of Food Gels

Material selection, molecular interactions, formulation, and processing determine whether a food gel develops as a nanogel, a microgel, or a macrogel. This section addresses the consequence of that outcome: why gels of similar composition behave differently when their structural scale changes. Three structural levers explain most of the differences: the surface-to-volume ratio together with the length over which molecules must diffuse; the way water is confined within the polymer mesh, the pores of the network, and the spaces between particles; and whether mechanical stress is carried by individual soft particles or by a continuous network [24]. The levers are coupled, since reducing size accelerates transport but also increases water exchange with the medium and the exposure of encapsulated compounds. Throughout this comparison, the terms nanogel, microgel, and macrogel refer to the characteristic external dimension of the gel object, as defined in Section 3.3.1. Each object contains internal scales (mesh, strands, pores, and domains), so the comparison concerns which length dominates a given property, not a hierarchy of mutually exclusive levels.

Figure 5 illustrates three of these consequences. In panel (a), water appears in three states, bound to the chains, trapped in the mesh, and free in a large pore, and part of it leaves the gel as syneresis. Panel (b) contrasts the two ways in which a gel carries stress: soft particles that deform and slide past each other under shear, and a continuous network that first bulges under compression and then breaks into irregular fragments. Panel (c) shows the four release routes, which do not follow one another but compete, and whose relative weight changes with the scale of the gel.

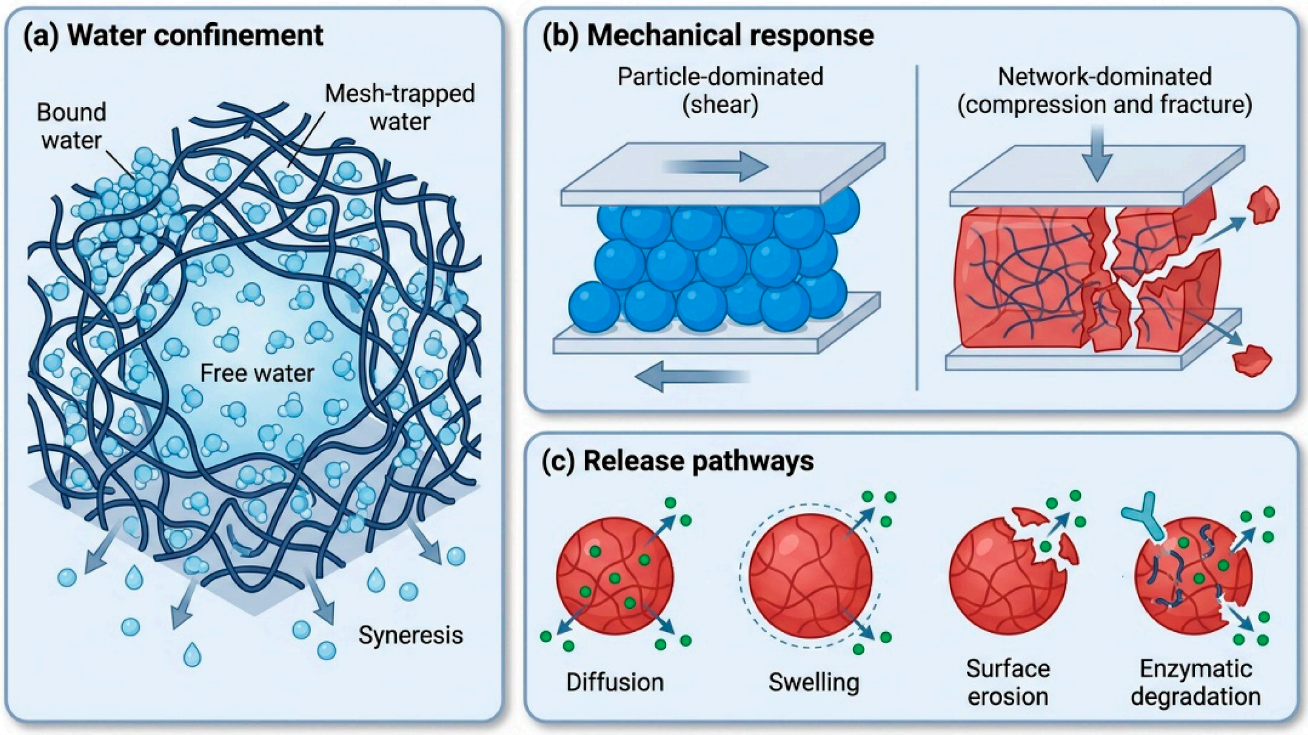


Figure 5. Scale-dependent properties of food gels: (**a**) water confinement and syneresis; (**b**) particle- versus network-dominated mechanical response; (**c**) release pathways (not to scale). Illustration generated with FigureLabs (figurelabs.ai) from concepts designed by the authors and subsequently checked and edited by them.

5.1. Surface-to-Volume Ratio and Mass Transport

The most direct effect of reducing structural scale is geometric. For a spherical gel particle, the surface-to-volume ratio equals $3/R$, where R is the radius: 3×10^3 m^{-1} for a bead with $R = 1$ mm, 6×10^4 m^{-1} for a microgel with $R = 50$ µm, and 6×10^7 m^{-1} for a nanogel with $R = 50$ nm. A nanogel therefore exposes approximately 2×10^4 times more surface per unit volume than a millimetric bead of the same composition, so a much larger fraction of its network contacts the medium: water, ions, and enzymes reach the interior more easily, and more of any encapsulated compound lies close to the surface. These features explain why nanogels are regarded as highly responsive carriers that can load both hydrophilic and hydrophobic compounds and react quickly to stimuli [14]. Scale also sets the characteristic diffusion time, which scales approximately as L^2/D, where L is the diffusion path length and D is the diffusion coefficient. For $D \approx 10^{-9}$ m^2 s^{-1}, typical of small solutes in water, diffusion across 1 mm takes approximately 10^3 s, across 50 µm approximately 2.5 s, and across 50 nm only a few microseconds. Within a gel, diffusivity is lower because the network obstructs molecular motion, so absolute times are longer. However, the quadratic dependence on size remains, and the three regimes differ by orders of magnitude [171]. The short diffusion paths of nanogels therefore cannot delay the release of small molecules on their own, and nanogels must rely on additional retention mechanisms.

The most important of these is the relationship between mesh size and solute size. Solutes much smaller than the mesh diffuse almost freely; as solute size approaches the mesh size, obstruction and hydrodynamic interactions markedly reduce diffusivity; and solutes larger than the mesh are physically entrapped and released only if the network swells, degrades, or erodes [172]. Because crosslinking density and swelling set the mesh size, the formulation variables that control structural scale also control transport. Electrostatic and hydrophobic solute–polymer affinity can reduce effective diffusivity well below steric expectations [173], and heterogeneous or particulate networks increase tortuosity and lengthen the path a molecule must follow [174]. These factors combine differently at each scale. In nanogels, rapid equilibration favors fast loading and rapid responses to pH, ionic strength, or temperature. However, it can also cause premature release unless the compound is retained by binding, a dense core, or a protective shell [81]. In microgels, solutes diffuse first through each particle and then through the fluid between particles. Hence, suspensions and packed or granular systems have an additional interparticle pathway tunable through particle size and packing [175]. In macrogels, diffusion across the bulk network limits transport, generating concentration gradients, an initial release dominated by near-surface regions, and slower sustained release from the interior [176]. Structural scale thus sets an upper limit on transport rates, while the actual rate depends on mesh size, solute–matrix affinity, tortuosity, swelling, and crosslinking density.

Figure 6 makes this quadratic dependence visible. Each tenfold reduction in path length shortens the diffusion time a hundredfold, which is why the three marked radii fall at microseconds, seconds, and about a quarter of an hour. The two dashed lines are just as telling: when the network slows diffusion by one or two orders of magnitude, a millimetric gel moves from minutes to hours, whereas a nanogel still equilibrates almost at once, so obstruction alone cannot turn a nanogel into a slow-release system.

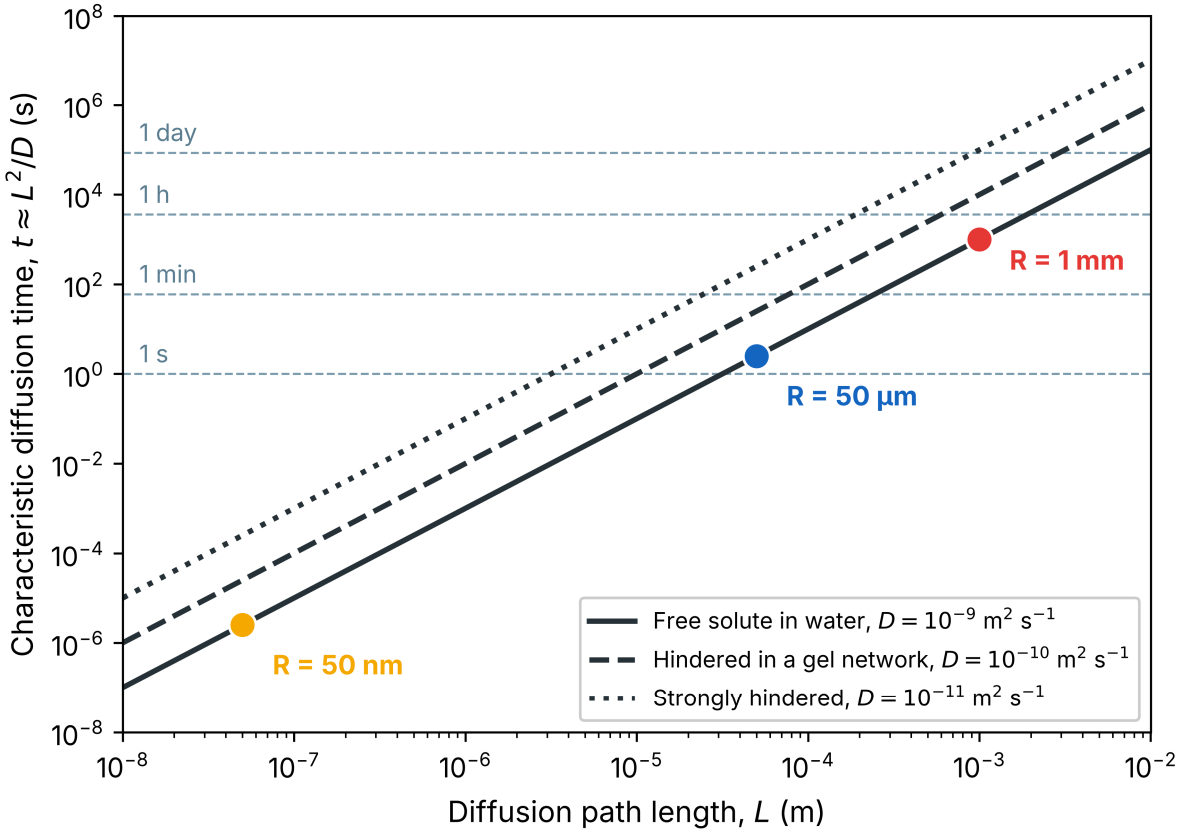


Figure 6. Characteristic diffusion time as a function of path length ($t \approx L^2/D$) for a free solute ($D = 10^{-9}$ m^2 s^{-1}) and two levels of hindrance within a gel network (10^{-10} and 10^{-11} m^2 s^{-1}). Original figure generated by the authors from the scaling relation discussed in [172]; plotted in Python (Matplotlib).

5.2. Water Confinement, Porosity, and Network Connectivity

Water in food gels is not a homogeneous phase: some interact closely with the polymer as hydration water, some is immobilized within the mesh or small pores, and some behaves almost as free water in larger pores or channels. Low-field nuclear magnetic resonance distinguishes these populations through their transverse relaxation times, with longer times generally reflecting more mobile water in larger spaces, although water exchange between populations and matrix composition require caution in interpretation [177]. Structural scale determines where water resides. In nanogels, almost all water lies within a small swollen mesh close to the chains; micrometer-scale pores are absent, and exchange with the medium is extremely fast. In microgels, water is distributed between the particle interior, where the network holds it, and interstitial spaces, where no continuous structure retains it, and it is more mobile and easily lost; in stirred acid milk gels, which consist of dispersed gel particles, syneresis has been related to particle rearrangement and to serum-filled regions monitored by LF-NMR and image analysis [178]. In macrogels, water occupies both the mesh and micrometer-scale pores and is retained through capillary, osmotic, and elastic contributions [6,24]. Figure 5a represents these three populations and the water lost through syneresis.

Water-holding capacity and permeability depend primarily on porosity and pore connectivity. Fine, uniform networks with small, evenly distributed pores generally retain water more effectively, while coarse, heterogeneous networks with large pores or serum channels release it more readily under stress or during storage [179]. Interconnected pores support fluid flow and solute transport, whereas isolated pores trap water. Because crosslinking density determines mesh size and equilibrium swelling, more densely crosslinked networks

swell less, retain less solvent, and are less permeable [172]. Granular hydrogels made from packed microparticles also have interconnected interparticle porosity, separate from each particle's mesh, which can be designed to facilitate transport [85].

Water confinement is also linked to storage stability [180]. Gel networks rarely reach equilibrium after formation, and strand contraction, particle fusion, or local coarsening can expel water; the balance between the osmotic pressure of the polymer and the elastic pressure of the network decides whether a gel remains swollen or undergoes syneresis, and osmotic effects are a major trigger of syneresis in gelatin gels [6]. This instability depends on scale. Macrogels lose water through visible syneresis and shrinkage; in particulate or microgel-based systems, syneresis is associated with particle size and structural openness [178]; and nanogel dispersions show no macroscopic syneresis but can deswell with pH, ionic strength, or temperature [56], their main storage limitation being colloidal instability and aggregation, which cause loss of nanoscale character [181]. In microgels, by contrast, swelling changes modify particle softness and the effective volume fraction [83]. The same features that determine water retention also govern stress transmission, since crosslinking density, connectivity, and heterogeneity control both water distribution and elastic response; in particulate networks, the heterogeneous organization of the solid matrix governs the viscoelastic spectrum [21], as discussed next.

5.3. Mechanical, Rheological, Textural, and Tribological Behavior

Mechanical behavior changes qualitatively with scale because the stress-bearing element is different. In macrogels, stress is transmitted through a continuous network, and connectivity, crosslinking density, strand thickness, and heterogeneity control the response; in nanogel and microgel dispersions, stress is carried by discrete soft particles, and volume fraction, softness, and interparticle interactions dominate, together with a large interfacial contribution [24,182]. This explains why materials of similar composition can behave as firm, cuttable solids, spoonable soft solids, or pourable fluids. Figure 5b illustrates this difference.

In macrogels, the small-deformation elastic modulus increases with polymer concentration, crosslinking density, and connectivity because more load-bearing junctions resist deformation. However, in particulate and heterogeneous networks, a hierarchical organization of fractal elements governs the response [21]. At large deformations, fracture stress and strain, yield behavior, and failure mode depend on the distribution of weak points, strand thickness, pore size, and fillers or phase-separated domains, which also determine instrumental texture attributes such as hardness, springiness, cohesiveness, and adhesiveness [183]; fine, homogeneous networks generally deform more before failure, whereas coarse, particulate networks fracture at lower strains. Because small-amplitude measurements do not capture these nonlinear events, large-amplitude oscillatory shear has become an important tool for relating strain hardening, softening, and breakdown to microstructure [184]. Large deformations also induce water release, as compression of coarse networks expels serum [185].

Microgel dispersions behave as viscous fluids at low volume fractions, with viscosity increasing with concentration and swelling [186]. As particles crowd, they touch, compress, facet, and interpenetrate, and because they are soft, they can be packed beyond the concentrations at which rigid particles would jam, forming soft solids with a yield stress [182]; above this stress they flow and show marked shear thinning as particles deform, rearrange, and slide past each other. Fluid gels behave as structured solids at rest but flow above a critical stress, and their storage modulus, viscosity, and linear viscoelastic range depend on biopolymer concentration, particle size and shape, and the amount of unordered chains at the particle surface; because these dispersions rest on reversible contacts between particles,

their structure breaks down under shear and rebuilds at rest, and their yield stress and modulus change with time and repeated shear through physical aging [75,187]. Emulsion-based systems follow the same scale-dependent classification, with bulk emulsion gels, emulsion gel particles, and fluid emulsion gels showing distinct structure–property relationships and suited to different applications [11]. This time-dependent recovery is useful in pumping, spreading, and extrusion-based three-dimensional (3D) printing [8,24]. Nanogels serve as versatile hydrophilic delivery systems for encapsulating compounds [14], but at high concentrations they also behave as soft colloids whose flow depends on deformability and interpenetration [182]. Nano- and microscale gel particles incorporated into continuous matrices can reinforce or weaken the composite depending on their interaction with the surrounding network, as with droplets and gel particles in filled and emulsion gels [188].

Structural scale also shapes texture perception and oral processing [11]. Macrogels are first fractured during mastication, so perceived firmness and cohesiveness depend on fracture behavior, whereas later stages depend increasingly on lubrication by fragments, saliva, and dispersed particles [70]. Soft protein microgels combine viscosity enhancement with good lubrication and have therefore been proposed as fat replacers in low-fat foods [3]; plant protein microgels obtained by shearing a percolated protein gel reduced boundary friction by about an order of magnitude compared with native proteins, with a lubrication performance comparable to that of an oil-in-water emulsion [17]. The rheological and tribological behavior of fluid gels likewise depends on particle size, shape, and surface structure, making them useful for texture modification, including foods for people with swallowing difficulties [52]. As gels become smaller, mechanical behavior thus shifts from network-dominated responses (shape, firmness, fracture-related texture) to particle-dominated ones (yield stress, shear thinning, creaminess, lubrication), with nanogels acting mainly through interfaces or as fillers and composites combining both [85,189]. The breakdown of these structures during processing, mastication, and digestion also determines the release of encapsulated compounds.

5.4. Encapsulation, Release, Stability, and Digestibility

Encapsulation efficiency depends on whether a compound is entrapped during gelation or loaded afterward by diffusion and partitioning and on how well the network retains it: molecules larger than the mesh remain physically trapped, whereas smaller ones are retained only if they interact with the polymer [190]. In nanogels, the large surface area places much of the load near the surface, favoring high loading capacity for both hydrophilic and hydrophobic compounds but making retention strongly dependent on binding [81]. Size also sets an absolute limit on what can be encapsulated: probiotic bacteria are generally entrapped in capsules and hydrogel beads ranging from micrometers to millimeters, whereas nanoscale structures are used as thin protective coatings around individual cells rather than as carriers that contain them [191]. Protein, polysaccharide, and mixed hydrogels have been widely used to deliver phenolic compounds, vitamins, and probiotics [192]. The four release routes discussed below are shown in Figure 5c.

Protection against light, oxygen, temperature, and the acidic gastric environment largely depends on barrier function: gel networks restrict the mobility of encapsulated compounds and the diffusion of oxygen, prooxidants, protons, and enzymes toward them, and well-designed hydrogels improve acid stability and bile salt resistance [192]. Because diffusion time increases with the square of path length, thicker matrices generally provide more effective barriers than nanoscale particles of the same composition: nanogels protect compounds mostly through molecular interactions and the local environment of their core, whereas microgels and macrogels also exploit longer diffusion paths. Thermal protection additionally depends on network stability, since thermoreversible physical gels may melt

during processing, whereas covalently crosslinked or thermoirreversible networks retain their integrity.

Release proceeds through diffusion through the network, swelling that enlarges the mesh, erosion of the gel surface, and chemical or enzymatic degradation of the network [172,192], and the dominant route depends on scale: in nanogels, diffusion is so fast that release is controlled mainly by binding and by triggers such as pH, ionic strength, or temperature that induce swelling or disassembly; in microgels, diffusion, swelling, and erosion operate on comparable time scales and can be balanced through size and crosslinking density; and in macrogels, near-surface diffusion is followed by erosion and fragmentation. Geometry matters too: during dynamic in vitro gastric digestion, whey protein gel spheres degraded mainly by surface erosion, whereas cubes fragmented first and then eroded, and larger cubes showed limited pepsin diffusion attributed to their lower specific surface area [96].

Enzyme access is one of the clearest scale-dependent effects. Because enzymes are macromolecules, their diffusion into gels is hindered far more than that of small solutes, and dense networks tend to be digested from the surface inward. Hence, the surface exposed to digestive fluids—which depends on initial gel size and on the fragments produced during mastication and gastric processing—largely controls hydrolysis [96]. Network architecture modulates the effect: in whey protein emulsion gels with similar droplet size, a hard, compact particulate gel disintegrated and was hydrolyzed more slowly during gastric digestion than a soft gel, which showed earlier droplet coalescence [140]. More generally, proteins and polysaccharides can assemble structures that encapsulate lipids and nutrients and modify gastrointestinal fluid properties, thereby modulating macronutrient digestion and bioavailability [193]. Bioaccessibility is the result. For lipophilic compounds, it is closely linked to lipid digestion, since the compounds must be released from the lipid phase and incorporated into mixed micelles; in the whey protein emulsion gels above, capsaicinoid bioaccessibility correlated with free fatty acid release [140]. Reducing scale usually increases the surface available for digestion and can improve the solubility and bioaccessibility of poorly soluble compounds, a key advantage of nanogels [14], but it may also cause premature gastric release. In contrast, larger or more densely crosslinked structures delay disintegration and shift release toward the intestine, which suits acid-sensitive compounds and probiotics but may reduce the fraction released if the matrix is insufficiently degraded [194,195].

Storage stability can be analyzed similarly. Chemical degradation such as oxidation depends on the ingress of oxygen and pro-oxidants and on exchange of the encapsulated compound with its surroundings, so it proceeds faster when diffusion paths are short and surfaces are large; in emulsion-based carriers, curcumin degraded faster during storage as droplet size decreased, attributed to faster exchange between the droplet interior and the aqueous phase [141], whereas entrapping oil droplets or carotenoids in biopolymer microgels has been reported to inhibit lipid oxidation and improve storage and thermal stability [196]. Physical instability, in turn, takes a different form at each scale, from syneresis in macrogels to aggregation in nanogel dispersions. Any design that accelerates transport for rapid release also tends to accelerate the entry of water, oxygen, and other reactive species during storage, so release and stability must be optimized together. Table 4 summarizes the comparison. No property favors the same scale throughout: the short diffusion paths that make nanogels fast and highly bioaccessible also expose their cargo during storage, and the continuous network that gives a macrogel its firmness also slows its digestion, so selecting a scale means selecting a set of trade-offs rather than an optimum.

Table 4. Comparison of scale-dependent properties of nanogels, microgels, and macrogels.

Property	Nanogels	Microgels	Macrogels	References
Dominant behavior	Surface-dominated colloidal carriers	Soft, deformable particles that pack, jam, and adsorb at interfaces	Continuous, space-spanning networks controlled by connectivity	[24,78,182]
Surface-to-volume ratio and diffusion time [a]	~6×10^7 m^{-1}; a few microseconds (R = 50 nm)	~6×10^4 m^{-1}; ~2.5 s (R = 50 µm)	~3×10^3 m^{-1}; ~10^3 s (R = 1 mm)	[172]
Control of mass transport	Binding interactions, dense cores or shells, and stimulus-triggered swelling	Intraparticle diffusion plus an interparticle pathway tuned by size and packing	Diffusion across the bulk network; concentration gradients and surface-dominated initial release	[14,85,172]
Water confinement	Water held close to the chains within a small mesh; very rapid exchange with the medium	Water inside particles and in interstitial spaces, where it is more easily lost	Water in the mesh and in micrometer-scale pores; syneresis when networks coarsen or contract	[6,177,178]
Mechanical and rheological behavior	Little effect on bulk rheology at typical concentrations; soft-colloid behavior when concentrated	Yield stress, shear thinning, jamming, and time-dependent recovery (e.g., fluid gels)	Elastic modulus, fracture, and texture attributes governed by network architecture	[21,52,182,183]
Oral processing and tribology	Mainly interfacial effects	Lubrication and creaminess; fat replacement	Fracture during mastication, followed by lubrication by fragments	[3,17,48]
Encapsulation	High loading of hydrophilic and hydrophobic compounds; retention depends on binding; too small to contain cells	Larger entities, including probiotic cells; tunable size and efficiency	Large loads; molecules larger than the mesh are physically entrapped	[14,172,197,198]
Release	Rapid; controlled mainly by binding and triggers (pH, ionic strength, temperature)	Diffusion, swelling, and erosion on comparable time scales	Surface diffusion followed by erosion and fragmentation; sustained release	[96,172,192]
Digestion and bioaccessibility	Large accessible surface; high bioaccessibility but risk of premature release	Intermediate behavior, adjustable through size and crosslinking	Surface-inward digestion; delayed release, with a risk of incomplete release	[14,96,140]
Storage stability	Aggregation; faster chemical degradation of labile compounds	Sedimentation or changes in swelling; microgel entrapment can inhibit oxidation	Syneresis and textural changes	[6,141,196]
Main food functions	Delivery and protection of bioactive compounds	Texture and mouthfeel, fat replacement, emulsion stabilization, and carriers	Bulk texture, shape, water retention, and sustained release	[3,97,192]

[a] Surface-to-volume ratio calculated as $3/R$; characteristic diffusion time estimated as L^2/D, with $L = R$, for a small solute with $D \approx 10^{-9}$ m^2 s^{-1}; actual times in gels are longer because the network hinders diffusion.

5.5. Critical Assessment of Evidence

Not all the relationships outlined above rest on equally strong evidence, and the distinction matters: structural scale can work as a design parameter only once it is clear which relationships hold reliably and which do not.

Some are well established. The geometric consequences of size—the increase in surface-to-volume ratio and the quadratic decrease in diffusion time—follow from first principles and are reported consistently across systems [172]. So do the dependence of solute transport on the solute-to-mesh size ratio and the reduction in mesh size with crosslinking density [172]. The distinction between fine-stranded and particulate protein networks and its dependence on the balance between attraction and repulsion has been reproduced in many protein systems [25,28]. Two further results are equally well reproduced: soft particles pack beyond the jamming limit of rigid colloids [79,182], and dense gels are digested from the surface inward, so the exposed area controls hydrolysis [96].

Other relationships are reported in opposite directions, usually because the same variable acts through competing mechanisms. Increasing crosslinker concentration enlarges particles by accelerating gelation during synthesis [137,138] but reduces the swollen size of formed networks [199]; therefore, results are comparable only when the measurement stage is specified. Shear generally reduces particle size [143,161], but it can also promote aggregation at low intensity [135] or leave size unchanged above a critical value [146]. Increasing biopolymer molecular weight can either protect proteins against uncontrolled aggregation or promote large, unstable aggregates, depending on charge and pH [94]. Reducing scale improves bioaccessibility while accelerating chemical degradation during storage [14,141,200], so reports of "improved performance" depend on which property is measured. Finally, researchers have described the elasticity of particulate gels using widely different scaling indices, which they attribute to a hidden hierarchical organization rather than a single structural variable [21].

Methodological heterogeneity further limits comparisons between studies. Particle size is reported as hydrodynamic diameter, image-based diameter, or scattering-derived radius, and these quantities are not equivalent, especially for soft, swollen, or irregular particles. Formulation and processing variables are rarely independent, since changing polymer concentration also changes viscosity, crosslinking density, and droplet size during emulsification; single-variable interpretations may therefore mislead. Many mechanisms have been demonstrated in synthetic or model systems, but their transfer to food-grade biopolymers, polydisperse and compositionally variable, has seldom been verified. Most structural characterization is conducted on dried or diluted samples rather than in situ, and few measurements have been made in real food matrices, during processing, or under digestion. These limitations do not invalidate the framework proposed here, but they define the conditions for applying its predictions and point to the need for standardized methods and in situ characterization.

A minimum in situ characterization protocol would improve comparability across scales. Studies should identify explicitly whether the reported length corresponds to hydrodynamic particle diameter, image-based particle size, mesh size, pore size, aggregate size, or phase-domain size; report measurements in the hydrated state whenever possible, together with pH, ionic strength, temperature, polymer concentration, and equilibration time; combine at least one structural technique (e.g., scattering, confocal microscopy, microtomography, or AFM) with rheological or mechanical measurements performed under matched conditions; report full size distributions rather than only mean values for polydisperse soft particles; and document sample preparation steps that can alter structure, particularly dilution, freezing, drying, staining, or solvent exchange. For dynamic systems, time-resolved or coupled methods such as rheo-SAXS/rheo-SANS are preferable because they can relate structural rearrangement directly to mechanical response. These

criteria would not eliminate differences among techniques, but they would make structural descriptors traceable and enable more meaningful cross-study comparisons. Because formulation and processing variables rarely change independently, parameters such as viscosity, droplet size, and crosslinking density should be quantified rather than assumed fixed, and mechanisms demonstrated in synthetic or model systems should be verified in food-grade biopolymers and, where feasible, in real food matrices, during processing, and under simulated digestion. Standardization criteria and emerging in situ techniques are discussed further in Section 7 [7,201].

6. Food Applications

The scale-dependent properties and design principles of each type of gel determine which type of gel suits a given application, so structural scale can be read as a level of functional design [4,192]. Macrogels are used when the gel itself constitutes the food structure, and its network properties are perceived directly as shape, firmness, and texture; microgels when dispersed soft particles are needed to modify mouthfeel, stabilize interfaces, or carry ingredients; and nanogels mainly when the objective is the protection and controlled release of sensitive compounds.

Figure 7 pairs each scale with its dominant structural feature, the property that results, and representative foods: nanogels, whose short diffusion paths favor protection and release, in functional beverages and capsules; microgels, acting as soft particles, in the creaminess of sauces and stirred yogurt; and macrogels, whose continuous protein network provides firmness and holds water, in sausages and tofu. The contrast is quantitative at comparable composition: a heat-set whey protein network fragments and is digested at a rate set by its elasticity [48], whereas proteins dispersed as microgels reduce boundary friction by about an order of magnitude [17], and as nanogel carriers they exchange storage stability for bioaccessibility because of their short diffusion paths [14,141].

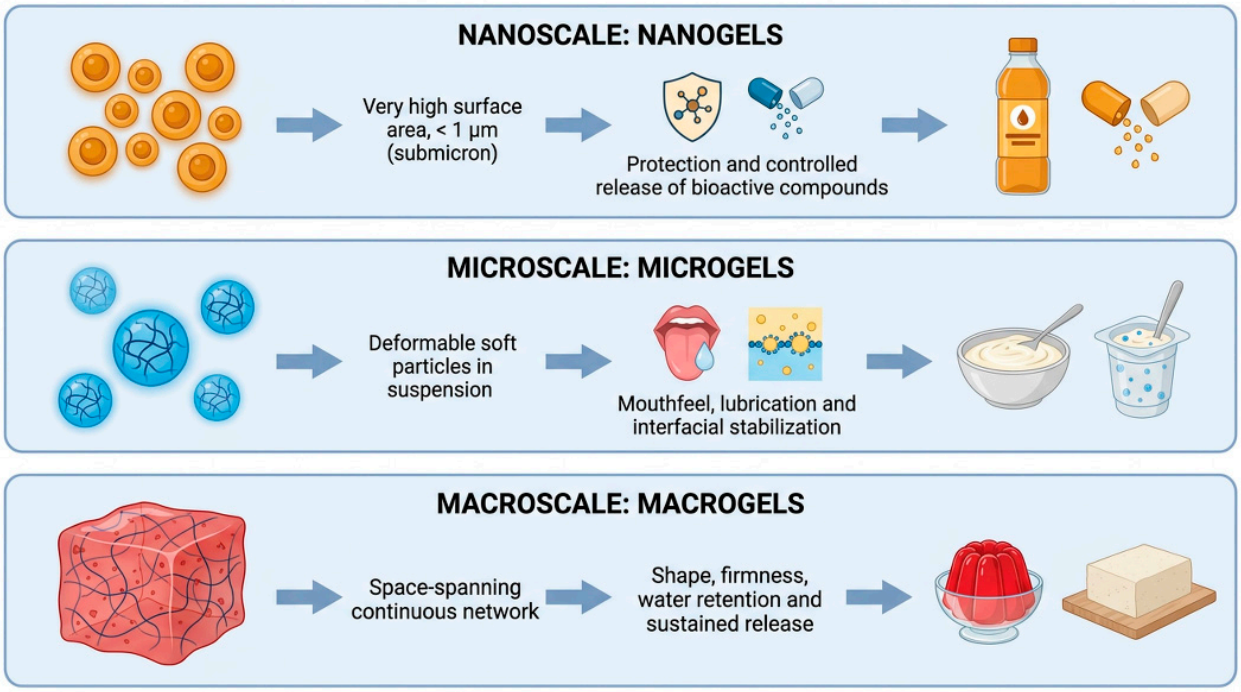


Figure 7. Characteristics of the types of gels applied to foods. Arrows indicate the sequence from each gel type to its main structural feature, the resulting functionality and representative food applications. Illustration generated with FigureLabs (figurelabs.ai) from concepts designed by the authors and subsequently checked and edited by them.

6.1. Macrogels: Bulk Texture, Shape, and Structural Functions

Macrogels are continuous gels with characteristic dimensions generally ranging from millimeters to centimeters and take the form of blocks, spheres, cylinders, films, fibers, foams, or porous structures. Because they form a continuous network, they suit direct texture structuring, water immobilization, shape retention, and protective functions [192]. They are therefore the obvious choice when the gel forms the main body of the food or an important structural phase: desserts, spoonable gels, jams, sauces, creams, yogurts, meat products and analogs, and gel-based composite foods.

Three application groups illustrate this role. In confectionery and dessert gels, hydrocolloid choice and gelation conditions determine firmness, elasticity, clarity, melting behavior, and flavor release, so pectin, agar, carrageenan, gelatin, and gellan yield products with markedly different sensory profiles [40]. The same architectural variables that govern texture also govern behavior during consumption: in heat-set whey protein gels, the more elastic gels formed at pH 7 fragmented into larger particles during simulated oral processing and were digested more slowly than the brittle gels obtained at pH 3 and 5, which broke into smaller particles and were hydrolyzed more rapidly [48]. Gel architecture therefore determines not only perceived texture but also the rate at which a product is digested. The macrogel's external dimension is a second lever. Whey protein gel cubes of 3.1, 5.2, and 10.3 mm and spheres of 6.5 mm broke down by different routes during dynamic gastric digestion, spheres mainly by erosion and cubes by fragmentation followed by erosion, and pepsin activity remaining in the liquid phase was highest with the largest cubes because their lower specific surface area limited enzyme diffusion into the particle [96]. For a product designed as a block, sphere, or film, size and shape therefore set digestion kinetics as much as the network does. In meat products and meat analogs, protein networks bind water and form cohesive structures, and the density and nature of protein–protein interactions determine hardness, elasticity, and water-holding capacity, which are central to developing next-generation analogs [202]. In dairy and gelled products, pore size, network connectivity, polymer concentration, and crosslinking control the mechanical response during mastication and therefore the perceived texture [183,203]. Macrogels are also used when a larger matrix is required to retain and release compounds slowly, as in calcium alginate beads or pectin and starch hydrogels designed for the colonic delivery of probiotics [192], or when a product needs a supporting structure with a defined shape, as within tailored sensory design, fat reduction, and 3D food printing [4].

6.2. Microgels: Mouthfeel, Emulsions, and Soft-Particle Structuring

Microgels are micrometer- or submicrometer-scale gel particles dispersed in a continuous phase that combine a hydrated internal network with colloidal behavior, allowing them to act as structuring particles, ingredient carriers, and interfacial elements [204]. Unlike bulk gels, they form fluid suspensions, respond rapidly to environmental changes, and deform at interfaces, making them suitable for foods that require colloidal functionality rather than a continuous gel block [205]. Protein microgels are soft, water-rich particles whose rheological and tribological behavior falls between that of native proteins and conventional gels.

Their first major application is fat replacement. Soft protein microgels based on whey, pea, egg white, or lactoferrin increase viscosity and improve lubrication, which makes them candidates for low-fat foods that require creaminess and low friction [3]. Microgels obtained by shearing a percolated plant protein gel reduced boundary friction by about an order of magnitude relative to the native proteins and matched the lubrication performance of a 20% oil-in-water emulsion, an effect that depended on microgel volume fraction [17]. The gain comes from the change in stress-bearing element rather than from composition: the native protein and the microgel share the same chemistry, but once the

protein is confined in discrete, deformable particles, stress is carried by particle deformation and sliding instead of by a continuous network (Section 5.3), which is why lubrication and creaminess emerge at the microscale while firmness belongs to the macroscale. Soy protein isolate–high-acyl gellan microgels, whose size, zeta potential, wettability, and rheology can be tuned through polysaccharide concentration, have been used to mimic the oral sensation of a fat phase in margarine- and mayonnaise-like products [206]. A second application is stabilizing emulsions and foams, because deformable microgels adsorb at oil–water and air–water interfaces and form thick viscoelastic layers that resist coalescence and ripening [78,166], a mechanism also reported for meat protein microgels with dual interfacial characteristics [207]. Related soft particles, such as starch granules, plant cells, and dairy microgels, already perform this function in many traditional foods, and microgels also control the texture of sauces, purées, and stirred yogurt, where particle size and softness determine mouthfeel [156]. Converting a polysaccharide into microgels can create functionality the polymer lacks in solution: agar and curdlan microgels conferred emulsifying ability on non-surface-active polysaccharides, and curdlan-stabilized emulsions resisted centrifugation better than agar ones, whereas gellan gum microgels showed no such effect [101]. Fluid gels extend the same principle to flow behavior, since biopolymer concentration and particle characteristics can adjust their yield stress and lubrication, a feature exploited in texture-modified foods for people with swallowing difficulties [208]. A third application is encapsulation at the colloidal scale: microgels entrap lipophilic compounds, antioxidants, and carotenoids within porous, hydrated particles, and mild fabrication methods allow accurate control of particle size plus encapsulation efficiency, an advantage for sustained-release systems [209]. Soy protein microgels obtained by thermal self-assembly or fragmentation and gelatin–gum arabic microcapsules loaded with lutein illustrate how these particles act simultaneously as Pickering stabilizers, carriers, and texture modifiers while improving stability against light, heat, and humidity [114,209]. Their size also makes them the only gel scale able to host probiotic cells, as in alginate–chitosan, carrageenan–caseinate, and pectin–gelatin microgels that protect the cells and control their release [210].

6.3. Nanogels: Delivery and Protection of Bioactive Compounds

Nanogels are the smallest class of gels, submicron in size and typically a few hundred nanometers, and combine a crosslinked network with a high surface area and a rapid response to changes in pH, temperature, or ionic conditions. They are therefore particularly suitable when foods require practically invisible carriers for sensitive compounds and are more useful for encapsulation and controlled release than for generating bulk texture [14]. Most applications target ingredients whose functionality is limited by low solubility, susceptibility to oxidation, degradation during processing, or low bioaccessibility, including vitamins, antioxidants, carotenoids, and other nutraceuticals [14].

Reported food uses include whey protein and protein–polysaccharide nanogels and milk protein nanohydrogels carrying antioxidants, as well as gelatin nanogel coatings with essential oils applied to fruits and vegetables, where they act both as delivery vehicles and as interfacial stabilizers that reduce moisture loss and microbial growth [4]. Ovalbumin gel nanoparticles loaded with carvacrol, with diameters of 40–60 nm by transmission electron microscopy, remained stable below 85 °C and at NaCl concentrations below 90 mM and released their load in two stages, with 12.1% in the first 60 h and 82.7% after 168 h; applied as a coating on fresh pork stored at 4 °C, they reduced weight loss by up to 43% and the loss of thiol groups by 26.8% relative to free carvacrol and kept lipid oxidation below the sensory threshold of 0.5 mg malondialdehyde per kilogram for 15 days [97]. Adjusting crosslinking density, composition, and sensitivity to pH, ionic strength, or digestive enzymes allows stimulus-responsive release during digestion [211]. Several reviews indicate that nanogels

and related nanostructures can improve bioavailability and enable pH-responsive release profiles [4,212]. Their short diffusion paths also require careful design to avoid premature release and degradation during storage, so the gain in bioaccessibility from reduced scale must be balanced against the loss of chemical stability [141]. Moving a single material across scales makes the trade-off concrete: wet pulverization of amylose gels containing ionic polysaccharides reduced the particles from 20–26 µm to nanofibrils of 240–670 nm, and the surface charge supplied by the polysaccharide kept these nanofibrils dispersed as a stable colloid, a function the micrometer-scale particles lacked [95]. Reducing scale therefore buys dispersibility and bioaccessibility at the cost of chemical protection, and nanogels are the right choice when the first two dominate the design briefly.

Table 5 summarizes representative applications by scale. The concentration of recent studies among microgel and nanogel applications, against the longer tradition of macrogel structuring in desserts, dairy foods, and meat products, reflects where the field is growing. The same alginate or protein appears at more than one scale, and what changes between applications is the structural function rather than the material, which is the practical consequence of treating scale as a design variable. Whey protein illustrates this directly: it forms sliceable heat-set gels whose texture and digestion rate are set by network architecture and external size [48,96], soft microgels that lubricate and replace fat [3,156], and nanogels that carry antioxidants [4]; alginate likewise forms calcium beads for colonic delivery [192] and microgels that host probiotic cells [210].

Table 5. Representative food applications of macrogels, microgels, and nanogels.

Scale	Application	Composition or Example	Structural Function	Reference
Macrogel	Gelatins, jellies, jams, desserts, and confectionery	Pectin, agar, carrageenan, gelatin, and gellan	The hydrocolloid and gelation conditions determine firmness, elasticity, clarity, melting, and flavor release.	[40]
Macrogel	Meat products and meat analogs	Protein networks that bind water and form cohesive structures in meat products, meat analogs, and restructured foods	The density and nature of protein–protein interactions determine hardness, elasticity, and water-holding capacity.	[202]
Macrogel	Texture modification in yogurt, cheese, dairy desserts, and gelled products	Gelling agents (e.g., agarose), thickeners (e.g., xanthan, alginate), co-solutes (sugars), and water	Pore size, network connectivity, polymer concentration, and crosslinking control the mechanical response during mastication	[183]
Macrogel	Nutrient delivery systems	Calcium alginate beads or matrices with vitamins, polyphenols, or probiotics; pectin/starch hydrogels for colonic delivery of probiotics	Combine structural and transport functions and control release during digestion.	[192]
Microgel	Encapsulation and protection of functional ingredients	Soy protein microgels obtained by thermal self-assembly or fragmentation; gelatin–gum arabic microcapsules with lutein; polysaccharide microgels for enzyme immobilization	Act as Pickering stabilizers, carriers, and texture modifiers and improve stability against light, heat, and humidity	[114,209]

Table 5. *Cont.*

Scale	Application	Composition or Example	Structural Function	Reference
Microgel	Probiotic carriers	Alginate–chitosan (*Lactobacillus rhamnosus* GG), carrageenan–caseinate (*Lactobacillus plantarum*), and pectin–gelatin (*Lactobacillus casei*) microgels	Protect cells and control their release; can be combined with proteins or metal ions to improve stability.	[210]
Microgel	Fat replacement in semisolid foods (margarine- and mayonnaise-like products)	Soy protein isolate–high-acyl gellan microgels with tunable size, zeta potential, wettability, and rheology	Reproduce the oral sensation of a fat phase	[206]
Microgel	Emulsion stabilization	Meat protein microgels with dual interfacial properties	Pickering-like stabilization of emulsions	[207]
Nanogel	Encapsulation of bioactive compounds	Whey protein and protein–polysaccharide nanogels; milk protein nanohydrogels carrying antioxidants; gelatin nanogel coatings with essential oils for fruits and vegetables	Delivery vehicles and interfacial stabilizers; coatings that reduce moisture loss and microbial growth	[4]
Nanogel	Shelf-life extension of meat	Ovalbumin gel nanoparticles of 40–60 nm loaded with carvacrol, applied as a coating on fresh pork.	Stable below 85 °C and 90 mM NaCl; two-stage release (12.1% at 60 h, 82.7% at 168 h); weight loss reduced by up to 43% and thiol loss by 26.8% versus free carvacrol	[97]
Nanogel	Controlled release and bioaccessibility	Nanogels with tuned crosslinking density, composition, and sensitivity to pH, ionic strength, or digestive enzymes	Stimuli-responsive release during digestion	[211]

7. Challenges and Future Trends

Advanced gelled systems for food applications remain largely at the basic and applied research stages, and transferring them to industry faces major challenges in characterization, scale-up, and sustainability [213]. Many studies have been conducted under specific experimental conditions and with methodologies that do not allow correlations among formulation, processing, structure, and functionality, so standardized databases will be necessary before artificial intelligence and machine learning tools can support predictive models for the rational design, scale-up, and application of these systems [7]. Development should also consider preparation stages, solvents, energy consumption, and processing operations, which may determine both techno-economic feasibility and environmental impact [213]. Below, we discuss the main challenges and perspectives related to predictive models, AI, industrial scale-up, sustainability, methodological standardization, and emerging characterization techniques.

Industrial scale-up is limited by the difficulty of quantitatively predicting gel behavior, as reproducible results and standardized processing conditions remain lacking, even though researchers have studied the nature and proportion of polymers, molecular interactions, and processing conditions that influence crosslinking, phase separation, and kinetic evolution [214]. The principal challenge lies in translating the structure–property–function relationship into a predictive instrument that covers both network architecture and reproducibility. Because nano-, micro-, and macrostructural scales coexist within the same gel,

scale-up should consider descriptors of structure, stability, release kinetics, functionality, and digestibility, and design will require the integration of predictive models, AI, multiscale characterization, experimental standardization, and sustainability [4].

Relationships among formulation, processing, and properties are typically elucidated through variables such as ionic strength, concentration, molecular weight, protein/polysaccharide ratio, temperature, shear, G′, hardness, syneresis, encapsulation efficiency, and diffusion kinetics; these results, however, are usually valid only under specific experimental conditions. To expand their predictive capability, models should integrate molecular and intermolecular descriptors (molecular weight, charge density, flexibility, hydrophobicity, and affinity between components), structural descriptors (aggregate size, porosity, anisotropy, connectivity, and fractal dimension), and functional responses (rheology, fracture, diffusion, water retention, compound release, and intestinal disintegration) [215], together with processing history, since changes in heating, cooling, residence time, mixing, or crosslinking may modify the network even when the formulation is unchanged.

AI and ML can analyze many possible combinations of proteins, polysaccharides, and lipids; their concentrations and proportions; pH; salt levels; crosslinking agents; and processing conditions, using rheological, microscopic, spectroscopic, and scattering data already generated. For meat-analog gels, Random Forest models and multilayer neural networks outperformed power-law and Cross equations, reaching R^2 values of 0.994–0.996 for viscosity prediction, consistent with the textural attributes of the final products [216]. Random Forest also predicted rheological parameters from 140 formulations of pea and faba bean proteins mixed with starch, pectin, cellulose, and carrageenan, and incorporating large-deformation parameters improved prediction of the nonlinear regime and revealed relationships not easily detected by conventional multivariate analysis [217]. Structural descriptors have also been mapped directly onto macroscopic rheology: topological, fractal, and texture descriptors extracted computationally from time-lapse super-resolution micrographs of acid-induced casein gelation reproduced the sol–gel transition detected by rheology and tracked the storage modulus, resolving network percolation and post-gelation rearrangements that bulk rheology averages out [218]. ML can thus integrate stability, microstructure, texture, and processability in complex colloidal systems [219]. AI should not, however, replace physicochemical knowledge: data-driven models may perform well within their training domain but fail when extrapolated to new raw materials or processing conditions, and when data are limited, hybrid models with physical constraints and uncertainty analysis should be used [220]. Because the literature contains fragmented data, different protocols, and non-equivalent units, FAIR databases that integrate composition, raw material origin, processing conditions, experimental protocols, rheological curves, microstructural images, and sensory properties will be necessary [221], making AI and methodological standardization inseparable challenges.

The transition from laboratory formulations to industrial production is another challenge for hydrogels, oleogels, aerogels, and hybrid systems [222–224]. Increasing process scale modifies thermal gradients, residence time, shear, mixing efficiency, mass transfer, and air incorporation, so chemically identical formulations may generate different structures, and critical process parameters must be identified that preserve the relationships among mixing, heat and mass transfer, and gelation rate, particularly when structure depends on phase separation, aggregation, or thermomechanical history. Aerogels illustrate this difficulty. In starch gels, freeze-drying produced materials with 92 ± 3% porosity that were mainly macroporous, with pores of approximately 20–100 μm and a maximum specific surface area of only 7.7 m^2/g, whereas supercritical CO_2 drying gave pores ≤1 μm and surface areas of 183–197 m^2/g, although shrinkage during ethanol exchange reduced porosity to 61–76% [225]. In cellulose nanofibers, supercritical drying gave lower densities and

specific surface areas of 72–115 m^2/g [226], whereas Ca^{2+}-crosslinked cellulose reached 296–331 m^2/g with lower shrinkage. However, freeze-dried cryogels showed compressive strength up to about twice as high [227]. In whey protein aerogels, supercritical CO_2 drying produced pores smaller than 1 μm and approximately 96% oil retention, against 45% in freeze-dried materials [228]. Scale-up therefore depends not on a universally superior technique but on balancing specific surface area, pore distribution, shrinkage, mechanical strength, and functionality against processing time and the demand and recovery of solvents and CO_2. Although continuous supercritical drying of particles has been demonstrated [229], techno-economic and life cycle analyses are still needed to quantify capital expenditure, operating expenditure, energy consumption, productivity, and cost per kilogram, and scale-up should be treated as a design constraint from the early stages rather than a later development phase.

This perspective is directly related to sustainability. Agro-industrial by-products offer opportunities to replace conventional materials and valorize waste streams [213,224], but their use does not guarantee a sustainable process, since extraction, purification, chemical modification, homogenization, freezing, drying, or solvent exchange may account for a significant fraction of the environmental impact. Green strategies should therefore incorporate life cycle assessment and techno-economic analyses with functional units related to technological application, such as the amount of structured oil, reduction in syneresis, mechanical stability, shelf-life extension, or encapsulated bioactive compounds. By-product valorization also introduces variability related to variety, maturity, region, season, or the previous industrial process, which may alter purity, molecular weight, and composition and thus affect gelation and reproducibility [224].

Standardized methods and characterization criteria will be essential to reduce this variability. Authors should specify whether terms such as nanogel, microgel, or macrogel refer to total particle size, aggregates, pore size, or phase domains, and report the origin, purity, moisture, molecular weight and its distribution, degree of substitution, surface charge, and particle size of materials, together with time–temperature relationships, pH, ionic concentration, agitator type, mixing speed, and storage conditions. In rheology, standardize the determination of the linear viscoelastic region and frequency and amplitude sweeps, and use nonlinear rheology via large-amplitude oscillatory shear to reveal strain hardening, softening, and rupture mechanisms that small-amplitude oscillatory shear does not detect [230].

Standardization should be complemented by techniques that link structure and behavior under conditions close to the gel's actual state. Scanning electron microscopy provides valuable morphological information but requires sample preparation or drying, whereas rheology evaluates the hydrated material; in situ characterization using small-angle X-ray scattering, small-angle neutron scattering, wide-angle X-ray scattering, and X-ray microtomography, and combinations such as rheo-SAXS or rheo-SANS, will therefore be necessary to observe structural reorganization and mechanical response simultaneously [201]. Low-field nuclear magnetic resonance, Raman and Fourier-transform infrared imaging, confocal microscopy, and atomic force microscopy can contribute to studying water mobility, local composition, interfaces, and heterogeneity [24,230]. Because these techniques generate larger data volumes than conventional characterization, they require automated image segmentation, descriptor extraction, dimensionality reduction, and multimodal data fusion; advanced characterization and AI should therefore be developed as components of a single platform integrating composition, processing, structure, properties, and function, together with scale-up and sustainability constraints [201,219]. This approach will enable the transition from experimental descriptions of gels to rational, reproducible design for food applications under complex industrial conditions.

8. Conclusions

Food gels are multiscale materials whose functionality depends not only on chemical composition but also on how their networks are organized from the molecular to the macroscopic level. This review proposes a framework in which structural scale is treated as a physicochemical design parameter linking formulation, gelation, and functional performance. Its contribution is to organize the field by structural scale rather than by material or application, compare the three scales property by property, and make explicit both the available quantitative evidence and its limitations. The nature of the building blocks, the type and kinetics of the interactions that connect them, and the degree to which network growth is confined or allowed to percolate determine whether a system develops as a nanogel, a microgel, or a macrogel. Polymer characteristics and formulation variables such as pH, ionic strength, concentration, crosslinking, and processing conditions such as shear, temperature, flow, and gelation rate together shape this outcome, mainly through competition among network growth, fragmentation, and kinetic arrest.

Once formed, each structural scale modifies the gel's physicochemical behavior in characteristic ways. Reducing size increases the surface-to-volume ratio and shortens diffusion paths, changes how water is confined, and shifts mechanical behavior from network-dominated to particle-dominated responses. The resulting division of roles (shape, firmness, and sustained release at the macroscale; soft-particle rheology, lubrication, interfacial activity, and the capacity to carry probiotic cells at the microscale; solubilization, protection, and stimulus-responsive release at the nanoscale) involves trade-offs, particularly between rapid release and storage stability, so hierarchical systems that combine several scales within one food structure appear especially promising [8].

Important challenges remain. The boundaries between nanogels, microgels, and macrogels are not standardized; many mechanisms have been demonstrated only in model or synthetic systems; and data obtained under different protocols are difficult to compare. Future studies should report structural descriptors consistently, combine in situ multiscale characterization with predictive and data-driven models, and consider scale-up and sustainability from early in the design process. Treating structural scale as an explicit design variable, together with a critical appraisal of the available evidence, can support the rational development of food gels with tailored texture, stability, and nutritional functionality.

Author Contributions: Conceptualization, S.A.O.-P.; methodology, S.A.O.-P.; investigation, S.A.O.-P., C.I.G.-B., A.U.-S., J.E.A.-T. and M.L.Z.-Z.; writing—original draft preparation, S.A.O.-P., C.I.G.-B., A.U.-S., J.E.A.-T. and M.L.Z.-Z.; writing—review and editing, S.A.O.-P., C.I.G.-B., A.U.-S., J.E.A.-T. and M.L.Z.-Z.; project administration, S.A.O.-P. All authors have read and agreed to the published version of the manuscript.

Funding: This research was funded by the Secretaría de Ciencia, Humanidades, Tecnología e Innovación (SECIHITI), grant number CBF-2026-2102; by the Programa Interno de Cátedras de Investigación (PICI) of the Facultad de Estudios Superiores Cuautitlán, Universidad Nacional Autónoma de México, grant numbers CI2640 and CI26103.

Data Availability Statement: No new data were created or analyzed in this study. Data sharing does not apply to this article.

Acknowledgments: The schematic illustrations (Figures 1, 2, 4, 5 and 7) were generated with FigureLabs (figurelabs.ai) from concepts and sketches designed by the authors. Figures 3 and 6 were plotted in Python (Matplotlib). All figures were checked and edited by the authors, who take full responsibility for their content.

Conflicts of Interest: The authors declare no conflicts of interest.

Abbreviations

The following abbreviations are used in this manuscript:

BSA	Bovine serum albumin
FTIR	Fourier-transform infrared
LAOS	Large-amplitude oscillatory shear
LF-NMR	Low-field nuclear magnetic resonance
pNIPAm	Poly(N-isopropylacrylamide)
SANS	Small-angle neutron scattering
SAOS	Small-amplitude oscillatory shear
SAXS	Small-angle X-ray scattering
SEM	Scanning electron microscopy
WAXS	Wide-angle X-ray scattering
WPI	Whey protein isolate

References

1. Zhi, L.; Liu, Z.; Wu, C.; Ma, X.; Hu, H.; Liu, H.; Adhikari, B.; Wang, Q.; Shi, A. Advances in preparation and application of food-grade emulsion gels. *Food Chem.* **2023**, *424*, 136399. [CrossRef] [PubMed]
2. Farahani, Z.K. A unified mechanistic perspective on protein–polysaccharide interactions underlying hybrid gel formation: A mini review. *Curr. Res. Food Sci.* **2026**, *12*, 101436. [CrossRef] [PubMed]
3. Kew, B.; Holmes, M.J.; Stieger, M.; Sarkar, A. Review on fat replacement using protein-based microparticulated powders or microgels: A textural perspective. *Trends Food Sci. Technol.* **2020**, *106*, 457–468. [CrossRef] [PubMed]
4. Yang, T.; Cao, L.; Song, J.; Skirtach, A.G. Tuning nanostructure of gels: From structural and functional controls to food applications. *Gels* **2025**, *11*, 620. [CrossRef] [PubMed]
5. Zheng, H.; Zhong, R.; Du, Y.; Liang, P.; Shi, F. Structural design and cutting-edge applications in food industry of food gels: A comprehensive review. *Food Res. Int.* **2026**, *231*, 118683. [CrossRef]
6. Nath, P.C.; Debnath, S.; Sridhar, K.; Inbaraj, B.S.; Nayak, P.K.; Sharma, M. A comprehensive review of food hydrogels: Principles, formation mechanisms, microstructure, and its applications. *Gels* **2023**, *9*, 1. [CrossRef] [PubMed]
7. Li, S.; Luo, M.; Boldianu, A.B.; McClements, D.J. Food-grade emulsion gels as nutrient delivery systems—Standardized workflow for fabrication, characterization, and application. *Gels* **2025**, *12*, 298. [CrossRef] [PubMed]
8. Liu, B.; Yang, H.; Zhu, C.; Xiao, J.; Cao, H.; Simal-Gandara, J.; Li, Y.; Fan, D.; Deng, J. A comprehensive review of food gels: Formation mechanisms, functions, applications, and challenges. *Crit. Rev. Food Sci. Nutr.* **2024**, *64*, 760–782. [CrossRef] [PubMed]
9. Khalesi, M.; Glenn-Davi, K.; Mohammadi, N.; FitzGerald, R.J. Key Factors Influencing Gelation in Plant vs. Animal Proteins: A Comparative Mini-Review. *Gels* **2023**, *10*, 575. [CrossRef] [PubMed]
10. Fu, K.; Wang, H.; Wang, H.; Pan, T.; Cai, Z.; Yang, Z.; Liu, D.; Wang, W. Gel-forming polysaccharides of traditional gel-like foods: Sources, structure, gelling mechanism, and advanced applications. *Food Res. Int.* **2024**, *198*, 115329. [CrossRef] [PubMed]
11. Liu, L.; Javed, H.U.; Xiao, J. Engineering emulsion gels as functional colloids emphasizing food applications: A review. *Front. Nutr.* **2022**, *9*, 890188. [CrossRef] [PubMed]
12. Ferdaus, J.; Mahmud, N.; Talukder, S.; da Silva, R.C. Characteristics and Functional Properties of Bioactive Oleogels: A Current Review. *Gels* **2025**, *11*, 69. [CrossRef] [PubMed]
13. McClements, D.J. Designing biopolymer microgels to encapsulate, protect and deliver bioactive components: Physicochemical aspects. *Adv. Colloid Interface Sci.* **2016**, *240*, 31–59. [CrossRef] [PubMed]
14. da Silva, M.P.; Fabi, J.P. Food biopolymers-derived nanogels for encapsulation and delivery of biologically active compounds: A perspective review. *Food Hydrocoll. Health* **2022**, *2*, 100079. [CrossRef]
15. Karg, M.; Pich, A.; Hellweg, T.; Hoare, T.R.; Lyon, L.A.; Crassous, J.J.; Suzuki, D.; Gumerov, R.A.; Schneider, S.; Potemkin, I.I.; et al. Nanogels and Microgels: From Model Colloids to Applications, Recent Developments, and Future Trends. *Langmuir* **2019**, *35*, 6231–6255. [CrossRef] [PubMed]
16. Martins, J.T.; Bourbon, A.I.; Pinheiro, A.C.; Fasolin, L.H.; Vicente, A.A. Protein-Based Structures for Food Applications: From Macro to Nanoscale. *Front. Sustain. Food Syst.* **2018**, *2*, 77. [CrossRef]
17. Kew, B.; Holmes, M.J.; Liamas, E.; Ettelaie, R.; Connell, S.D.; Dini, D.; Sarkar, A. Transforming sustainable plant proteins into high performance lubricating microgels. *Nat. Commun.* **2023**, *14*, 4743. [CrossRef] [PubMed]
18. Di Lorenzo, F.; Hellwig, J.; von Klitzing, R.; Seiffert, S. Macroscopic and Microscopic Elasticity of Heterogeneous Polymer Gels. *ACS Macro Lett.* **2015**, *4*, 698–703. [CrossRef] [PubMed]
19. Chen, W.; Cheng, H. Food Gels: Fabrication, Characterization, and Application. *Gels* **2025**, *11*, 886. [CrossRef] [PubMed]

20. Gentile, L. Protein–polysaccharide interactions and aggregates in food formulations. *Curr. Opin. Colloid Interface Sci.* **2020**, *48*, 18–27. [CrossRef]
21. Bantawa, M.; Keshavarz, B.; Geri, M.; Bouzid, M.; Divoux, T.; McKinley, G.H.; Del Gado, E. The hidden hierarchical nature of soft particulate gels. *Nat. Phys.* **2023**, *19*, 1178–1184. [CrossRef]
22. Smith, A.; Donley, G.J.; Del Gado, E.; Zavala, V.M. Topological Data Analysis for Particulate Gels. *ACS Nano* **2024**, *18*, 28622–28635. [CrossRef] [PubMed]
23. Wang, Q.; Chen, T.; Yan, S.; Li, Y.; Qi, B. Segregative phase separation of protein/polysaccharide mixed systems: Phase separation mechanisms, characterization technologies, influencing factors, and food applications—A review. *Food Res. Int.* **2025**, *208*, 116240. [CrossRef] [PubMed]
24. Cao, Y.; Mezzenga, R. Design principles of food gels. *Nat. Food* **2020**, *1*, 106–118. [CrossRef] [PubMed]
25. Nicolaï, T.; Durand, D. Controlled food protein aggregation for new functionality. *Curr. Opin. Colloid Interface Sci.* **2013**, *18*, 249–256. [CrossRef]
26. Banerjee, S.; Bhattacharya, S. Food Gels: Gelling Process and New Applications. *Crit. Rev. Food Sci. Nutr.* **2011**, *52*, 334–346. [CrossRef] [PubMed]
27. Cao, Y.; Mezzenga, R. Food protein amyloid fibrils: Origin, structure, formation, characterization, applications and health implications. *Adv. Colloid Interface Sci.* **2019**, *269*, 334–356. [CrossRef] [PubMed]
28. Nicolaï, T.; Britten, M.; Schmitt, C. β-Lactoglobulin and WPI aggregates: Formation, structure and applications. *Food Hydrocoll.* **2011**, *25*, 1945–1962. [CrossRef]
29. Duconseille, A.; Astruc, T.; Quintana, N.; Meersman, F.; Santé-Lhoutellier, V. Gelatin structure and composition linked to hard capsule dissolution: A review. *Food Hydrocoll.* **2014**, *43*, 360–376. [CrossRef]
30. An, D.; Ban, Q.; Du, H.; Wang, Q.; Teng, F.; Li, L.; Xiao, H. Nanofibrils of food-grade proteins: Formation mechanism, delivery systems, and application evaluation. *Compr. Rev. Food Sci. Food Saf.* **2022**, *21*, 4847–4871. [CrossRef] [PubMed]
31. Lucey, J.A. Acid Coagulation of Milk. In *Advanced Dairy Chemistry: Volume 1B: Proteins: Applied Aspects*, 4th ed.; McSweeney, P.L.H., O'Mahony, J.A., Eds.; Springer: New York, NY, USA, 2016; pp. 309–328. [CrossRef]
32. Li, Z.; Regenstein, J.M.; Teng, F.; Li, Y. Tofu products: A review of their raw materials, processing conditions, and packaging. *Compr. Rev. Food Sci. Food Saf.* **2020**, *19*, 3683–3714. [CrossRef] [PubMed]
33. Day, L. Proteins from land plants—Potential resources for human nutrition and food security. *Trends Food Sci. Technol.* **2013**, *32*, 25–42. [CrossRef]
34. Batool, Z.; Ahmed, S.; Hu, G.; Shen, B. Protein–polyphenol interactions in plant-based systems: Mechanisms, structure–function relationships, and nutritional implications. *Food Chem.* **2026**, *516*, 149387. [CrossRef] [PubMed]
35. Mishyna, M.; Keppler, J.K.; Chen, J. Techno-functional properties of edible insect proteins and effects of processing. *Curr. Opin. Colloid Interface Sci.* **2021**, *56*, 101508. [CrossRef]
36. Lanza, R.F.; Muccio, E.; Malvano, F.; Darvishikolour, M.; Marra, F.; Campanella, O.H.; Albanese, D. Tuning Gelation of Insect Proteins: Effect of Ionic Strength on Acheta domesticus Protein Extracts. *Gels* **2025**, *11*, 937. [CrossRef] [PubMed]
37. Mohan, K.; Udayarajan, C.T.; Fabra, M.J.; López-Rubio, A.; Nisha, P. Edible oleogels based on high molecular weight oleogelators and its prospects in food applications. *Crit. Rev. Food Sci. Nutr.* **2022**, *64*, 4432–4455. [CrossRef] [PubMed]
38. Rhein-Knudsen, N.; Meyer, A.S. Chemistry, gelation, and enzymatic modification of seaweed food hydrocolloids. *Trends Food Sci. Technol.* **2021**, *109*, 608–621. [CrossRef]
39. Said, N.S.; Olawuyi, I.F.; Lee, W.Y. Pectin Hydrogels: Gel-Forming Behaviors, Mechanisms, and Food Applications. *Gels* **2022**, *9*, 732. [CrossRef] [PubMed]
40. Saha, D.; Bhattacharya, S. Hydrocolloids as thickening and gelling agents in food: A critical review. *J. Food Sci. Technol.* **2010**, *47*, 587–597. [CrossRef] [PubMed]
41. Scott, G.; Awika, J.M. Effect of protein–starch interactions on starch retrogradation and implications for food product quality. *Compr. Rev. Food Sci. Food Saf.* **2023**, *22*, 2081–2111. [CrossRef] [PubMed]
42. Qosim, N.; Dai, Y.; Williams, G.R.; Edirisinghe, M.J. Structure, properties, forming, and applications of alginate fibers: A review. *Int. Mater. Rev.* **2024**, *69*, 309–333. [CrossRef]
43. Manzoor, S.; Masoodi, F.A.; Naqash, F.; Rashid, R. Oleogels: Promising alternatives to solid fats for food applications. *Food Hydrocoll. Health* **2022**, *2*, 100058. [CrossRef]
44. Arita-Merino, N.; te Nijenhuis, L.; van Valenberg, H.J.F.; Scholten, E. Multiple phase transitions and microstructural rearrangements shape milk fat crystal networks. *J. Colloid Interface Sci.* **2021**, *607*, 1050–1060. [CrossRef] [PubMed]
45. da Silva, T.L.T.; Martini, S. Recent Advances in Lipid Crystallization in the Food Industry. *Annu. Rev. Food Sci. Technol.* **2024**, *15*, 355–379. [CrossRef] [PubMed]
46. An, J.; Yang, F.; Zheng, L.; Yang, T. Structural Engineering of Edible Oleogels: From Molecular Assembly to Functional Food Applications. *Gels* **2026**, *12*, 649. [CrossRef] [PubMed]

47. Cerqueira, M.A.; Fasolin, L.H.; Picone, C.S.F.; Pastrana, L.; Cunha, R.L.; Vicente, A.A. Structural and mechanical properties of organogels: Role of oil and gelator molecular structure. *Food Res. Int.* **2017**, *96*, 161–170. [CrossRef] [PubMed]
48. Homer, S.; Williams, R.; Williams, A.; Logan, A. WPI gel microstructure and mechanical behaviour and their influence on the rate of in vitro digestion. *Foods* **2021**, *10*, 1066. [CrossRef] [PubMed]
49. Huang, Y.; Liu, J.; Zhu, Y.; Sun, B.; Liu, L.; Mngshou, L.; Zheng, B.; Li, Y.; Zhu, X. Physicochemical and gelling properties of heat-induced gels formed by soy lipophilic protein with β-conglycinin and glycinin. *Food Chem. X* **2025**, *29*, 102819. [CrossRef] [PubMed]
50. Cao, L.; Lu, W.J.; Mata, A.; Nishinari, K.; Fang, Y. Egg-box model-based gelation of alginate and pectin: A review. *Carbohydr. Polym.* **2020**, *242*, 116389. [CrossRef] [PubMed]
51. Descallar, F.B.A.; Yang, X.; Geonzon, L.C.; Matsukawa, S. Network structure and molecular mechanisms of food gels viewed from macroscopic, microscopic and molecular levels. *Food Sci. Technol. Res.* **2022**, *29*, 171–195. [CrossRef]
52. Ghebremedhin, M.; Seiffert, S.; Vilgis, T.A. Physics of agarose fluid gels: Rheological properties and microstructure. *Curr. Res. Food Sci.* **2021**, *4*, 436–448. [CrossRef] [PubMed]
53. Morris, E.R.; Nishinari, K.; Rinaudo, M. Gelation of gellan—A review. *Food Hydrocoll.* **2012**, *28*, 373–411. [CrossRef]
54. Nasatto, P.L.; Pignon, F.; Silveira, J.L.M.; Duarte, M.E.R.; Noseda, M.D.; Rinaudo, M. Methylcellulose, a Cellulose Derivative with Original Physical Properties and Extended Applications. *Polymers* **2015**, *7*, 777–803. [CrossRef]
55. Sacco, P.; Cok, M.; Asaro, F.; Paoletti, S.; Donati, I. The role played by the molecular weight and acetylation degree in modulating the stiffness and elasticity of chitosan gels. *Carbohydr. Polym.* **2018**, *196*, 405–413. [CrossRef] [PubMed]
56. Muñana-González, S.; Veloso-Fernández, A.; Ruiz-Rubio, L.; Pérez-Álvarez, L.; Vilas-Vilela, J.L. Covalent cross-linking as a strategy to prepare water-dispersible chitosan nanogels. *Polymers* **2022**, *15*, 434. [CrossRef] [PubMed]
57. Katashima, T. Precise Rheological Analysis of Permanently and Transiently Crosslinked Polymer Networks with Well-Controlled Structures. *Nihon Reoroji Gakkaishi* **2023**, *51*, 273–280. [CrossRef]
58. Zhu, W.; Hou, L.; Wu, P. On the molecular mechanism of thermally reversible sol–gel transition with pronounced hysteresis of agarose in water. *Soft Matter* **2025**, *21*, 7091–7099. [CrossRef] [PubMed]
59. Ghorbani, F.; Ghalandari, B.; Liu, Z.; Li, D.; Yu, B. Injectable light-assisted thermo-responsive methylcellulose-sodium humate hydrogel proposed for photothermal ablation and localized delivery of cisplatin. *Front. Bioeng. Biotechnol.* **2022**, *10*, 967438. [CrossRef] [PubMed]
60. Pratt, L.R. Molecular Theory of Hydrophobic Effects: "She is too mean to have her name repeated". *Annu. Rev. Phys. Chem.* **2002**, *53*, 409–436. [CrossRef] [PubMed]
61. Wijaya, W.; Patel, A.R.; Setiowati, A.D.; Van der Meeren, P. Functional colloids from proteins and polysaccharides for food applications. *Trends Food Sci. Technol.* **2017**, *68*, 56–69. [CrossRef]
62. Mezzenga, R.; Fischer, P. The self-assembly, aggregation and phase transitions of food protein systems in one, two and three dimensions. *Rep. Prog. Phys.* **2012**, *76*, 46601. [CrossRef] [PubMed]
63. Israelachvili, J.N. *Intermolecular and Surface Forces*, 3rd ed.; Academic Press: Burlington, MA, USA, 2011.
64. Narine, S.S.; Marangoni, A.G. Mechanical and structural model of fractal networks of fat crystals at low deformations. *Phys. Rev. E Stat. Phys. Plasmas Fluids Relat. Interdiscip. Top.* **1999**, *60*, 6991–7000. [CrossRef] [PubMed]
65. Nicolaï, T. Formation and functionality of self-assembled whey protein microgels. *Colloids Surf. B Biointerfaces* **2015**, *137*, 32–38. [CrossRef] [PubMed]
66. Kieliszek, M.; Misiewicz, A. Microbial transglutaminase and its application in the food industry. A review. *Folia Microbiol.* **2013**, *59*, 241–250. [CrossRef] [PubMed]
67. Zaidel, D.N.A.; Chronakis, I.S.; Meyer, A.S. Enzyme catalyzed oxidative gelation of sugar beet pectin: Kinetics and rheology. *Food Hydrocoll.* **2011**, *28*, 130–140. [CrossRef]
68. Rose, K.A.; Marino, E.; O'Bryan, C.S.; Murray, C.B.; Lee, D.; Composto, R.J. Nanoparticle dynamics in hydrogel networks with controlled defects. *Soft Matter* **2022**, *18*, 9045–9056. [CrossRef] [PubMed]
69. Grahn, P.; Lassila, P.; Valoppi, F. Micromechanical finite element modeling of crystalline lipid-based materials: Monoglyceride-based oleogels and their composites. *Mater. Horiz.* **2024**, *12*, 3358–3367. [CrossRef] [PubMed]
70. Gallego, M.; Baviera, J.M.B.; Grau, R.; Talens, P. Compositional, structural design and nutritional aspects of texture-modified foods for the elderly. *Trends Food Sci. Technol.* **2021**, *119*, 152–163. [CrossRef]
71. Tavagnacco, L.; Chiessi, E.; Severini, L.; Franco, S.; Buratti, E.; Capocefalo, A.; Brasili, F.; Conte, A.M.; Missori, M.; Angelini, R.; et al. Molecular origin of the two-step mechanism of gellan aggregation. *Sci. Adv.* **2023**, *9*, eadg4392. [CrossRef] [PubMed]
72. Onyianta, A.J.; Castellano, M.; Dorris, M.; Williams, R.; Vicini, S. The effects of morpholine pre-treated and carboxymethylated cellulose nanofibrils on the properties of alginate-based hydrogels. *Carbohydr. Polym.* **2018**, *198*, 320–327. [CrossRef] [PubMed]
73. Glover, Z.J.; Francis, M.J.; Bisgaard, A.L.H.; Andersen, U.; Johansen, L.B.; Povey, M.; Holmes, M.; Brewer, J.R.; Simonsen, A.C. Dynamic moisture loss explored through quantitative super-resolution microscopy, spatial micro-viscosity and macroscopic analyses in acid milk gels. *Food Hydrocoll.* **2019**, *101*, 105501. [CrossRef]

74. Hoefler, K.; Sukop, U.; Reiter, E.; Bender, D.; Jekle, M.; Roch, P.; Cichna-Markl, M.; D'Amico, S.; Schöenlechner, R. Comparative Characterization of Oxidative Enzymes for Arabinoxylan and Protein Cross-Linking via Ferulic Acid and Tyrosine in Model Systems. *J. Agric. Food Chem.* **2025**, *73*, 32183–32194. [CrossRef] [PubMed]
75. D'Oria, G.; Zeng, X.; Limbach, H.J.; Hartmann, C.; Ahrné, L.; Gunes, D.Z. Effect of stirring speed on low acyl gellan gum fluid gels' rheology, particle morphology and physical ageing. *Food Hydrocoll.* **2023**, *149*, 109614. [CrossRef]
76. Aufderhorst-Roberts, A.; Hughes, M.D.G.; Hare, A.; Head, D.; Kapur, N.; Brockwell, D.J.; Dougan, L. Reaction Rate Governs the Viscoelasticity and Nanostructure of Folded Protein Hydrogels. *Biomacromolecules* **2020**, *21*, 4253–4260. [CrossRef] [PubMed]
77. Suzuki, D. Nanogel/Microgel Science and Beyond. *Langmuir* **2023**, *39*, 7525–7529. [CrossRef] [PubMed]
78. Murray, B.S. Microgels at fluid-fluid interfaces for food and drinks. *Adv. Colloid Interface Sci.* **2019**, *271*, 101990. [CrossRef] [PubMed]
79. Vlassopoulos, D.; Cloître, M. Tunable rheology of dense soft deformable colloids. *Curr. Opin. Colloid Interface Sci.* **2014**, *19*, 561–574. [CrossRef]
80. Graham, N.; Cameron, A. Nanogels and microgels: The new polymeric materials playground. *Pure Appl. Chem.* **1998**, *70*, 1271–1275. [CrossRef]
81. Delgado-Pujol, E.J.; Martínez, G.; Casado-Jurado, D.; Vázquez, J.; León-Barberena, J.; Rodríguez-Lucena, D.; Torres, Y.; Alcudia, A.; Begines, B. Hydrogels and Nanogels: Pioneering the Future of Advanced Drug Delivery Systems. *Pharmaceutics* **2025**, *17*, 215. [CrossRef] [PubMed]
82. Mauri, E.; Perale, G.; Rossi, F. Nanogel Functionalization: A Versatile Approach To Meet the Challenges of Drug and Gene Delivery. *ACS Appl. Nano Mater.* **2018**, *1*, 6525–6541. [CrossRef]
83. Scheffold, F. Pathways and challenges towards a complete characterization of microgels. *Nat. Commun.* **2020**, *11*, 4315. [CrossRef] [PubMed]
84. Zhang, H.; Tumarkin, E.; Peerani, R.; Nie, Z.; Sullan, R.M.A.; Walker, G.C.; Kumacheva, E. Microfluidic Production of Biopolymer Microcapsules with Controlled Morphology. *J. Am. Chem. Soc.* **2006**, *128*, 12205–12210. [CrossRef] [PubMed]
85. Daly, A.C.; Riley, L.; Segura, T.; Burdick, J.A. Hydrogel microparticles for biomedical applications. *Nat. Rev. Mater.* **2020**, *5*, 20–43. [CrossRef] [PubMed]
86. Skjåk-Bræk, G.; Grasdalen, H.; Smidsrød, O. Inhomogeneous polysaccharide ionic gels. *Carbohydr. Polym.* **1989**, *10*, 31–54. [CrossRef]
87. Destribats, M.; Lapeyre, V.; Wolfs, M.; Sellier, E.; Leal-Calderon, F.; Ravaine, V.; Schmitt, V. Soft microgels as Pickering emulsion stabilisers: Role of particle deformability. *Soft Matter* **2011**, *7*, 7689. [CrossRef]
88. Stading, M.; Langton, M.; Hermansson, A. Small and large deformation studies of protein gels. *J. Rheol.* **1995**, *39*, 1445–1450. [CrossRef]
89. Dickinson, E. Emulsion gels: The structuring of soft solids with protein-stabilized oil droplets. *Food Hydrocoll.* **2011**, *28*, 224–241. [CrossRef]
90. Farjami, T.; Madadlou, A. An overview on preparation of emulsion-filled gels and emulsion particulate gels. *Trends Food Sci. Technol.* **2019**, *86*, 85–94. [CrossRef]
91. Hebishy, E.; Du, H.; Brito-Oliveira, T.C.; Pinho, S.C.; Miao, S. Saltiness perception in gel-based food systems (gels and emulsion-filled gels). *Crit. Rev. Food Sci. Nutr.* **2023**, *65*, 457–474. [CrossRef] [PubMed]
92. Shakeel, A.; Farooq, U.; Iqbal, T.; Yasin, S.; Lupi, F.R.; Gabriele, D. Key characteristics and modelling of bigels systems: A review. *Mater. Sci. Eng. C* **2018**, *97*, 932–953. [CrossRef] [PubMed]
93. Akgonullu, D.Z.; Murray, B.S.; Connell, S.D.; Yuan, F.; Linter, B.R.; Sarkar, A. Synthetic and biopolymeric microgels: Review of similarities and difference in behaviour in bulk phases and at interfaces. *Adv. Colloid Interface Sci.* **2023**, *320*, 102983. [CrossRef] [PubMed]
94. Du, J.; Cho, Y.-H.; Murphy, R.W.; Jones, O.G. Impact of Chitosan Molecular Weight and Attached Non-Interactive Chains on the Formation of α-Lactalbumin Nanogel Particles. *Gels* **2017**, *3*, 14. [CrossRef] [PubMed]
95. Suzuki, S.; Nishioka, J.; Kitamura, S. Characterization of Amylose Nanogels and Microgels Containing Ionic Polysaccharides. *J. Appl. Glycosci.* **2017**, *64*, 21–25. [CrossRef] [PubMed]
96. Mennah-Govela, Y.A.; Bornhorst, G.M. Breakdown mechanisms of whey protein gels during dynamic in vitro gastric digestion. *Food Funct.* **2021**, *12*, 2112–2125. [CrossRef] [PubMed]
97. Zhang, R.; Xu, G.; Su, Y.; Rao, S. Potential Application of Ovalbumin Gel Nanoparticles Loaded with Carvacrol in the Preservation of Fresh Pork. *Gels* **2023**, *9*, 941. [CrossRef] [PubMed]
98. Chyzy, A.; Tomczykowa, M.; Plonska-Brzezinska, M.E. Hydrogels as Potential Nano-, Micro- and Macro-Scale Systems for Controlled Drug Delivery. *Materials* **2020**, *13*, 188. [CrossRef] [PubMed]
99. Zhao, L.; Zhou, Y.; Zhang, J.; Liang, H.; Chen, X.; Tan, H. Natural Polymer-Based Hydrogels: From Polymer to Biomedical Applications. *Pharmaceutics* **2023**, *15*, 2514. [CrossRef] [PubMed]

100. Damiri, F.; Fatimi, A.; Paiva-Santos, A.C.; Varma, R.S.; Berrada, M. Smart stimuli-responsive polysaccharide nanohydrogels for drug delivery: A review. *J. Mater. Chem. B* **2023**, *11*, 10538–10565. [CrossRef] [PubMed]
101. Ishii, T.; Matsumiya, K.; Aoshima, M.; Matsumura, Y. Microgelation imparts emulsifying ability to surface-inactive polysaccharides: Bottom-up vs top-down approaches. *npj Sci. Food* **2018**, *2*, 15. [CrossRef] [PubMed]
102. Hughes, M.D.G.; Cussons, S.; Mahmoudi, N.; Brockwell, D.J.; Dougan, L. Tuning Protein Hydrogel Mechanics through Modulation of Nanoscale Unfolding and Entanglement in Postgelation Relaxation. *ACS Nano* **2022**, *16*, 10667–10678. [CrossRef] [PubMed]
103. Chander, S.; Kulkarni, G.T.; Dhiman, N.; Kharkwal, H. Protein-Based Nanohydrogels for Bioactive Delivery. *Front. Chem.* **2021**, *9*, 573748. [CrossRef] [PubMed]
104. Rusu, A.G.; Chiriac, A.P.; Nita, L.E.; Roșca, I.; Pinteală, M.; Mititelu-Tarțău, L. Chitosan Derivatives in Macromolecular Co-assembly Nanogels with Potential for Biomedical Applications. *Biomacromolecules* **2020**, *21*, 4231–4243. [CrossRef] [PubMed]
105. del Valle, L.J.; Díaz, A.; Puiggalí, J. Hydrogels for Biomedical Applications: Cellulose, Chitosan, and Protein/Peptide Derivatives. *Gels* **2017**, *3*, 27. [CrossRef] [PubMed]
106. Jin, B.; Zhou, X.; Li, X.; Lin, W.; Chen, G.; Qiu, R. Self-Assembled Modified Soy Protein/Dextran Nanogel Induced by Ultrasonication as a Delivery Vehicle for Riboflavin. *Molecules* **2016**, *21*, 282. [CrossRef] [PubMed]
107. Ruiz-Dávila, C.E.; Solís-Andrade, K.I.; Olvera-Sosa, M.; Palestino, G.; Rosales-Mendoza, S. Core-shell chitosan/Porphyridium-exopolysaccharide microgels: Synthesis, properties, and biological evaluation. *Int. J. Biol. Macromol.* **2023**, *246*, 125655. [CrossRef] [PubMed]
108. Azari-Anpar, M.; Degraeve, P.; Ecochard, S.; Jahanbin, K.; Assifaoui, A.; Adt, I.; Demarigny, Y.; Yazdi, F.T.; Oulahal, N. Effect of the interaction of nisin Z with various polysaccharides on its antibacterial activity. *Food Control* **2023**, *152*, 109874. [CrossRef]
109. Nourmohammadi, N.; Austin, L.; Chen, D. Protein-Based Fat Replacers: A Focus on Fabrication Methods and Fat-Mimic Mechanisms. *Foods* **2023**, *12*, 957. [CrossRef] [PubMed]
110. Akgonullu, D.Z.; O'Hagan, N.M.; Murray, B.S.; Connell, S.D.; Yuan, F.; Linter, B.R.; Sarkar, A. Bulk and Interfacial Behavior of Potato Protein-Based Microgels. *Langmuir* **2024**, *40*, 21341–21351. [CrossRef] [PubMed]
111. Gagliardi, A.; Giuliano, E.; Eeda, V.; Fresta, M.; Bulotta, S.; Awasthi, V.; Cosco, D. Biodegradable Polymeric Nanoparticles for Drug Delivery to Solid Tumors. *Front. Pharmacol.* **2021**, *12*, 601626. [CrossRef] [PubMed]
112. Marsili, L.; Bo, M.D.; Berti, F.; Toffoli, G. Chitosan-Based Biocompatible Copolymers for Thermoresponsive Drug Delivery Systems: On the Development of a Standardization System. *Pharmaceutics* **2021**, *13*, 1876. [CrossRef] [PubMed]
113. Harsányi, A.; Kardos, A.; Xavier, P.; Campbell, R.A.; Varga, I. A Novel Approach for the Synthesis of Responsive Core–Shell Nanogels with a Poly(N-Isopropylacrylamide) Core and a Controlled Polyamine Shell. *Polymers* **2024**, *16*, 2584. [CrossRef] [PubMed]
114. Matsumiya, K.; Murray, B.S. Soybean protein isolate gel particles as foaming and emulsifying agents. *Food Hydrocoll.* **2016**, *60*, 206–215. [CrossRef]
115. Han, M.; Liu, K.; Liu, X.; Rashid, M.T.; Zhang, H.; Wang, M. Research Progress of Protein-Based Bioactive Substance Nanoparticles. *Foods* **2023**, *12*, 2999. [CrossRef] [PubMed]
116. Ji, L.; Cornacchia, L.; Sala, G.; Scholten, E. Lubrication behavior of mixed colloidal systems: Effect of interactions between polysaccharides and oil droplets/protein particles. *Food Hydrocoll.* **2023**, *149*, 109584. [CrossRef]
117. Zhang, T.; Yang, R.; Yang, S.; Guan, J.; Zhang, D.; Ma, Y.; Liu, H. Research progress of self-assembled nanogel and hybrid hydrogel systems based on pullulan derivatives. *Drug Deliv.* **2018**, *25*, 278–292. [CrossRef] [PubMed]
118. Liu, Q.; Ma, D.; Cheng, H.; Yang, K.; Hou, B.; Heng, Z.; Qian, Y.; Liu, W.; Chen, S. pH-Responsive Nanogels from Bioinspired Comb-like Polymers with Hydrophobic Grafts for Effective Oral Delivery. *Gels* **2025**, *11*, 806. [CrossRef] [PubMed]
119. Moncho-Jordá, A.; Dzubiella, J. Swelling of ionic microgel particles in the presence of excluded-volume interactions: A density functional approach. *Phys. Chem. Chem. Phys.* **2015**, *18*, 5372–5385. [CrossRef] [PubMed]
120. Zheng, B.; Avni, Y.; Andelman, D.; Podgornik, R. Charge Regulation of Polyelectrolyte Gels: Swelling Transition. *Macromolecules* **2023**, *56*, 5217–5224. [CrossRef]
121. Portnov, I.V.; Larina, A.A.; Gumerov, R.A.; Potemkin, I.I. Swelling and Collapse of Cylindrical Polyelectrolyte Microgels. *Polymers* **2022**, *14*, 5031. [CrossRef] [PubMed]
122. Wang, C.; Liu, X.; Zhang, Y.; Li, X.; Ge, Y.; Lan, W.; Yang, L. Novel Blueberry Leaf Polysaccharide–Xanthan Gum Composite Gels for Curcumin Encapsulation: Enhanced Stability and Controlled Release. *Foods* **2025**, *14*, 2825. [CrossRef] [PubMed]
123. Pieper, M.I.; Mathews, H.F.; Pich, A. Ionic strength-induced compartmentalization for nanogel-in-microgel colloids. *Small* **2024**, *21*, 2410221. [CrossRef] [PubMed]
124. Chremos, A.; Horkay, F.; Douglas, J.F. Influence of network defects on the conformational structure of nanogel particles: From "closed compact" to "open fractal" nanogel particles. *J. Chem. Phys.* **2022**, *156*, 94903. [CrossRef] [PubMed]
125. Ferreira, S.A.; Pereira, P.; Sampaio, P.; Coutinho, P.J.G.; Gama, M. Supramolecular assembled nanogel made of mannan. *J. Colloid Interface Sci.* **2011**, *361*, 97–108. [CrossRef] [PubMed]

126. Jamard, M.; Sheardown, H.D. Effect of Methylcellulose Molecular Weight on the Properties of Self-Assembling MC-g-PNtBAm Nanogels. *Bioengineering* **2018**, *5*, 39. [CrossRef] [PubMed]
127. Maiz–Fernández, S.; Pérez-Álvarez, L.; Ruiz-Rubio, L.; González, R.P.; Sáez-Martínez, V.; Pérez, J.; Vilas-Vilela, J.L. Synthesis and Characterization of Covalently Crosslinked pH-Responsive Hyaluronic Acid Nanogels: Effect of Synthesis Parameters. *Polymers* **2019**, *11*, 742. [CrossRef] [PubMed]
128. Sultana, F.; Imran-Ul-Haque, M.d.; Arafat, M.; Sharmin, S. An Overview of Nanogel Drug Delivery System. *J. Appl. Pharm. Sci.* **2013**, *3*, S95–S105. [CrossRef]
129. Riederer, M.S.; Requist, B.D.; Payne, K.A.; Way, J.D.; Krebs, M.D. Injectable and microporous scaffold of densely-packed, growth factor-encapsulating chitosan microgels. *Carbohydr. Polym.* **2016**, *152*, 792–801. [CrossRef] [PubMed]
130. Wypysek, S.K.; Scotti, A.; Alziyadi, M.O.; Potemkin, I.I.; Denton, A.R.; Richtering, W.H. Tailoring the Cavity of Hollow Polyelectrolyte Microgels. *Macromol. Rapid Commun.* **2019**, *41*, 1900422. [CrossRef] [PubMed]
131. Giussi, J.M.; Velasco, M.I.; Longo, G.S.; Acosta, R.H.; Azzaroni, O. Unusual temperature-induced swelling of ionizable poly(N-isopropylacrylamide)-based microgels: Experimental and theoretical insights into its molecular origin. *Soft Matter* **2015**, *11*, 8879–8886. [CrossRef] [PubMed]
132. Li, C.; Obireddy, S.R.; Lai, W. Preparation and use of nanogels as carriers of drugs. *Drug Deliv.* **2021**, *28*, 1594–1602. [CrossRef] [PubMed]
133. Alghzzawy, Z.M.; Awwad, M.H.; Elmaghraby, T.K.; Hagag, S.A.E.-H.; Kayed, A.E.; Ghobashy, M.M.; Elbarbary, A.M.; Ibrahim, D.S. Development of pH-responsive gelatin/PVP nanogel by gamma radiation for controlled delivery of silibinin. *Sci. Rep.* **2026**, *16*, 19614. [CrossRef] [PubMed]
134. Logigan, C.-L.; Delaite, C.; Popa, M.; Băcăiţă, E.S.; Tiron, C.E.; Peptu, C.; Peptu, C.A.; Peptu, C.A.; Peptu, C.A. Poly(ethylene glycol) Methyl Ether Acrylate-Grafted Chitosan-Based Micro- and Nanoparticles as a Drug Delivery System for Antibiotics. *Polymers* **2024**, *16*, 144. [CrossRef] [PubMed]
135. Liu, P.; Pearce, C.M.; Anastasiadi, R.-M.; Resmini, M.; Castilla, A.M. Covalently Crosslinked Nanogels: An NMR Study of the Effect of Monomer Reactivity on Composition and Structure. *Polymers* **2019**, *11*, 353. [CrossRef] [PubMed]
136. Shoukat, H.; Pervaiz, F.; Khan, M.; Rehman, S.; Akram, F.; Abid, U.; Noreen, S.; Nadeem, M.; Qaiser, R.; Ahmad, R.; et al. Development of β-cyclodextrin/polyvinypyrrolidone-co-poly (2-acrylamide-2-methylpropane sulphonic acid) hybrid nanogels as nano-drug delivery carriers to enhance the solubility of Rosuvastatin: An in vitro and in vivo evaluation. *PLoS ONE* **2022**, *17*, e0263026. [CrossRef] [PubMed]
137. Salinas, Y.; Castilla, A.M.; Resmini, M. An l-proline based thermoresponsive and pH-switchable nanogel as a drug delivery vehicle. *Polym. Chem.* **2018**, *9*, 2271–2280. [CrossRef]
138. Whiteley, Z.; Ho, H.M.K.; Gan, Y.X.; Panariello, L.; Gkogkos, G.; Gavriilidis, A.; Craig, D.Q.M. Microfluidic synthesis of protein-loaded nanogels in a coaxial flow reactor using a design of experiments approach. *Nanoscale Adv.* **2021**, *3*, 2039–2055. [CrossRef] [PubMed]
139. Spencer, D.S.; Shodeinde, A.B.; Beckman, D.W.; Luu, B.C.; Hodges, H.R.; Peppas, N.A. Biodegradable cationic nanogels with tunable size, swelling and pKa for drug delivery. *Int. J. Pharm.* **2020**, *588*, 119691. [CrossRef] [PubMed]
140. Luo, N.; Ye, A.; Wolber, F.M.; Singh, H. Effect of Gel Structure on the In Vitro Gastrointestinal Digestion Behaviour of Whey Protein Emulsion Gels and the Bioaccessibility of Capsaicinoids. *Molecules* **2021**, *26*, 1379. [CrossRef] [PubMed]
141. Kharat, M.; Aberg, J.; Dai, T.; McClements, D.J. Comparison of Emulsion and Nanoemulsion Delivery Systems: The Chemical Stability of Curcumin Decreases as Oil Droplet Size Decreases. *J. Agric. Food Chem.* **2020**, *68*, 9205–9212. [CrossRef] [PubMed]
142. Foster, N.C.; Allen, P.; El Haj, A.J.; Grover, L.M.; Moakes, R.J.A. Tailoring therapeutic responses via engineering microenvironments with a novel synthetic fluid gel. *Adv. Healthc. Mater.* **2020**, *10*, 2100622. [CrossRef] [PubMed]
143. Boujemaa, M.; Peters, R.; Luan, J.; Mok, Y.H.; Keller, S.; Wilson, D.A. A simple vortex-based method for the generation of high-throughput spherical micro- and nanohydrogels. *Int. J. Mol. Sci.* **2025**, *26*, 6300. [CrossRef] [PubMed]
144. Maity, S.; Mahata, K.; Meshram, B.; Banerjee, S. Smart polymer-derived injectable hydrogels: Current status and future perspectives. *ACS Polym. AU* **2025**, *5*, 680–711. [CrossRef] [PubMed]
145. Smit, W.J.; Gibaud, T.; Manneville, S.; Divoux, T. Imprinting macroscopic fracture during gelation: A mechanism for tuning colloidal gels. *Phys. Rev. Mater.* **2026**, *10*, 045602. [CrossRef]
146. Bauland, J.; Wooster, T.J.; Fischer, P.; Vermant, J. Thermo-Rheological Memory of κ-Carrageenan Fluid Gels Formed under Flow. *Biomacromolecules* **2026**, *27*, 3352–3358. [CrossRef] [PubMed]
147. Farrés, I.F.; Norton, I.T. Formation kinetics and rheology of alginate fluid gels produced by in-situ calcium release. *Food Hydrocoll.* **2014**, *40*, 76–84. [CrossRef]
148. Das Anthuparambil, N.; Girelli, A.; Timmermann, S.; Kowalski, M.; Akhundzadeh, M.S.; Retzbach, S.; Senft, M.D.; Dargasz, M.; Gutmüller, D.; Hiremath, A.; et al. Exploring non-equilibrium processes and spatio-temporal scaling laws in heated egg yolk using coherent X-rays. *Nat. Commun.* **2023**, *14*, 5580. [CrossRef] [PubMed]

149. Liu, H.; Lionello, C.; Westley, J.; Cardellini, A.; Huynh, U.; Pavan, G.M.; Thayumanavan, S. Understanding functional group and assembly dynamics in temperature responsive systems leads to design principles for enzyme responsive assemblies. *Nanoscale* **2021**, *13*, 11568–11575. [CrossRef] [PubMed]
150. Farrés, I.F.; Moakes, R.J.A.; Norton, I.T. Designing biopolymer fluid gels: A microstructural approach. *Food Hydrocoll.* **2014**, *42*, 362–372. [CrossRef]
151. Vite, G.; Lopez-Godoy, S.; Díaz-Leyva, P.; Kozina, A. Improving the size distribution of polymeric oblates fabricated by the emulsion-in-gel deformation method. *Colloids Interfaces* **2022**, *7*, 50. [CrossRef]
152. Khatami, N.; Guerrero, P.; Caba, K.; Abarrategi, A.; Camarero-Espinosa, S. Chitosan- and gelatin-based composite granular hydrogels for cartilage tissue regeneration. *Int. J. Mol. Sci.* **2025**, *27*, 2889. [CrossRef] [PubMed]
153. Cheng, L.; Godfrin, P.D.; Swan, J.W.; Doyle, P.S. Thermal processing of thermogelling nanoemulsions as a route to tune material properties. *Soft Matter* **2018**, *14*, 5604–5614. [CrossRef] [PubMed]
154. Demirkır, Ç.; Wood, J.A.; Lohse, D.; Krug, D. Life beyond Fritz: On the detachment of electrolytic bubbles. *arXiv* **2024**, arXiv:2406.01989. [CrossRef]
155. Sivakumaran, D.; Bakaic, E.; Campbell, S.B.; Xu, F.; Mueller, E.; Hoare, T.R. Fabricating Degradable Thermoresponsive Hydrogels on Multiple Length Scales via Reactive Extrusion, Microfluidics, Self-assembly, and Electrospinning. *J. Vis. Exp.* **2018**, *134*, e54502. [CrossRef]
156. Lacroix, A.; Hayert, M.; Bosc, V.; Menut, P. Batch versus microfluidic emulsification processes to produce whey protein microgel beads from thermal or acidic gelation. *J. Food Eng.* **2021**, *312*, 110738. [CrossRef]
157. Yonet-Tanyeri, N.; Amer, M.S.; Balmert, S.C.; Korkmaz, E.; Falo, L.D.; Little, S.R. Microfluidic Systems For Manufacturing of Microparticle-Based Drug-Delivery Systems: Design, Construction, and Operation. *ACS Biomater. Sci. Eng.* **2022**, *8*, 2864–2877. [CrossRef] [PubMed]
158. Luo, Y.; Xu, R.; Hu, Z.; Ni, R.; Zhu, T.; Zhang, H.; Zhu, Y. Gel-Based Suspension Medium Used in 3D Bioprinting for Constructing Tissue/Organ Analogs. *Gels* **2024**, *10*, 644. [CrossRef] [PubMed]
159. Goswami, R.; Kim, K.; Boccaccini, A.R.; Guck, J.; Girardo, S. Fine-tuning cell-mimicking polyacrylamide microgels: Sensitivity to microscale reaction conditions in droplet microfluidics. *Mater. Des.* **2026**, *262*, 115450. [CrossRef]
160. Ji, W.; Chang, B.; Yu, H.; Li, Y.; Song, W. Effect of Polymer and Crosslinker Concentration on Static and Dynamic Gelation Behavior of Phenolic Resin Hydrogel. *Gels* **2024**, *10*, 325. [CrossRef] [PubMed]
161. Cooke, M.E.; Rosenzweig, D.H. The rheology of direct and suspended extrusion bioprinting. *APL Bioeng.* **2021**, *5*, 011502. [CrossRef] [PubMed]
162. Ashfaq, A.; Clochard, M.-C.; Coqueret, X.; Dispenza, C.; Driscoll, M.S.; Ulański, P.; Al-Sheikhly, M.I. Polymerization Reactions and Modifications of Polymers by Ionizing Radiation. *Polymers* **2020**, *12*, 2877. [CrossRef] [PubMed]
163. Miyata, T. Polymeric soft materials with molecular recognition: From static binding to dynamic functions in gels, particles, and interfaces. *Sci. Technol. Adv. Mater.* **2026**, *27*, 2664156. [CrossRef] [PubMed]
164. Mastella, P.; Moscardini, A.; Guerrini, A.; Luin, S. Fast assembly of 'clickable nanogels' for drug delivery. *Nanoscale Adv.* **2025**, *7*, 5421–5434. [CrossRef] [PubMed]
165. Minina, E.S.; Sánchez, P.A.; Likos, C.N.; Kantorovich, S.S. Studying synthesis confinement effects on the internal structure of nanogels in computer simulations. *J. Mol. Liq.* **2019**, *289*, 111066. [CrossRef]
166. Lefroy, K.S.; Murray, B.S.; Ries, M.E. Advances in the use of microgels as emulsion stabilisers and as a strategy for cellulose functionalisation. *Cellulose* **2021**, *28*, 647–670. [CrossRef]
167. Biswas, S.; Mukherjee, B.; Chakrabarti, B. Thermodynamics predicts a stable microdroplet phase in polymer-gel mixtures undergoing elastic phase separation. *arXiv* **2021**, arXiv:2104.00651. [CrossRef]
168. Oevreeide, I.H.; Szydlak, R.; Luty, M.; Ahmed, H.; Prot, V.; Skallerud, B.H.; Zemła, J.; Lekka, M.; Stokke, B.T. On the determination of mechanical properties of aqueous microgels: Towards high-throughput characterization. *Gels* **2021**, *7*, 64. [CrossRef] [PubMed]
169. Tobita, H. Application of Network Dimension Theory to the Kinetics of Nanogel Formation in Miniemulsion Vinyl/Divinyl Copolymerization: Free-Radical and Living Polymerization. *Macromol. React. Eng.* **2024**, *19*, 2400014. [CrossRef]
170. Rovers, M.M.; Rogkoti, T.; Bakker, B.K.; Bakal, K.J.; van Genderen, M.H.P.; Manuel, S.-S.; Dankers, P.Y.W. Using a Supramolecular Monomer Formulation Approach to Engineer Modular, Dynamic Microgels, and Composite Macrogels. *Adv. Mater.* **2024**, *36*, 2405868. [CrossRef] [PubMed]
171. Lin, X.; Wang, X.; Zeng, L.; Wu, Z.L.; Guo, H.; Hourdet, D. Stimuli-Responsive Toughening of Hydrogels. *Chem. Mater.* **2021**, *33*, 7633–7656. [CrossRef]
172. Richbourg, N.R.; Peppas, N.A. The swollen polymer network hypothesis: Quantitative models of hydrogel swelling, stiffness, and solute transport. *Prog. Polym. Sci.* **2020**, *105*, 101243. [CrossRef]
173. Alaa Eddine, M. Porous PEGDA/PEG Hydrogel Membranes: Permeability, Filtration and Structure. Ph.D. Thesis, Sorbonne Université, Paris, France, 2023. Available online: https://theses.hal.science/tel-04056846 (accessed on 12 October 2026).

174. Xue, C.; Huang, Y.; Zheng, X.; Hu, G. Hopping Behavior Mediates the Anomalous Confined Diffusion of Nanoparticles in Porous Hydrogels. *J. Phys. Chem. Lett.* **2022**, *13*, 10612–10620. [CrossRef] [PubMed]
175. O'Bryan, C.S.; Rose, K.A.; Ford, J.; Ghoto, M.R.; Lee, D.; Composto, R.J. Cross-Linking Density Controls the Interstitial Pore Size and Elasticity in Polyacrylamide Microgel Packings. *Macromolecules* **2025**, *58*, 3937–3948. [CrossRef]
176. Fatimi, A.; Okoro, O.V.; Podstawczyk, D.A.; Simińska-Stanny, J.; Shavandi, A. Natural Hydrogel-Based Bio-Inks for 3D Bioprinting in Tissue Engineering: A Review. *Gels* **2022**, *8*, 179. [CrossRef] [PubMed]
177. Gilbert, A.; Turgeon, S.L. Unraveling microstructure and water behavior in diverse food matrices using low-frequency NMR (LF-NMR) on proton: A specific look at 1H-LF-NMR results interpretation. *Food Hydrocoll.* **2025**, *172*, 111974. [CrossRef]
178. Gilbert, A.; Rioux, L.; St-Gelais, D.; Turgeon, S.L. Characterization of syneresis phenomena in stirred acid milk gel using low frequency nuclear magnetic resonance on hydrogen and image analyses. *Food Hydrocoll.* **2020**, *106*, 105907. [CrossRef]
179. Foudazi, R.; Zowada, R.; Manas-Zloczower, I.; Feke, D.L. Porous Hydrogels: Present Challenges and Future Opportunities. *Langmuir* **2023**, *39*, 2092–2111. [CrossRef] [PubMed]
180. Zhang, H.; Xia, T.; Chen, R.; Zhang, L.; Wang, X.; Ma, H.; Chai, Y.; Ren, Z.; Ji, J.; Ma, X.; et al. Confined Water Dynamics in Topological Networks Hydrogel for Aqueous Electrochemical Devices. *Small* **2024**, *21*, 2408819. [CrossRef] [PubMed]
181. Pinelli, F.; Saadati, M.; Zare, E.N.; Makvandi, P.; Masi, M.; Sacchetti, A.; Rossi, F. A perspective on the applications of functionalized nanogels: Promises and challenges. *Int. Mater. Rev.* **2022**, *68*, 1–25. [CrossRef]
182. Scotti, A.; Schulte, M.F.; Lopez, C.G.; Crassous, J.J.; Bochenek, S.; Richtering, W.H. How Softness Matters in Soft Nanogels and Nanogel Assemblies. *Chem. Rev.* **2022**, *122*, 11675–11700. [CrossRef] [PubMed]
183. Hu, B.; Zhang, Y.; Han, L.; Zhao, Y.; Zhang, C.; Cao, J.; Yang, J.; Fang, Y. Large deformation of food gels: Influencing factors, theories, models, and applications—A review. *Food Res. Int.* **2025**, *204*, 115933. [CrossRef] [PubMed]
184. Wang, Y.; Selomulya, C. Food rheology applications of large amplitude oscillation shear (LAOS). *Trends Food Sci. Technol.* **2022**, *127*, 221–244. [CrossRef]
185. Mollenkopf, P.; Kochanowski, J.A.; Ren, Y.; Vining, K.H.; Janmey, P.A.; Purohit, P.K. Poroelasticity and permeability of fibrous polymer networks under compression. *Soft Matter* **2024**, *21*, 2400–2412. [CrossRef] [PubMed]
186. Gury, L.; Gauthier, M.; Suau, J.; Vlassopoulos, D.; Cloître, M. Internal Microstructure Dictates Yielding and Flow of Jammed Suspensions and Emulsions. *ACS Nano* **2025**, *19*, 14931–14940. [CrossRef] [PubMed]
187. Malkin, A.Y.a.; Derkach, S.R.; Куличихин, В.Г. Rheology of Gels and Yielding Liquids. *Gels* **2023**, *9*, 715. [CrossRef] [PubMed]
188. Jiang, Y.; Cui, Y.; Li, Y.; Liu, Z.; Ness, C.; Seto, R. Filled colloidal gel rheology: Strengthening, stiffening, and tunability. *J. Rheol.* **2024**, *69*, 35–44. [CrossRef]
189. Lin, D.; Kelly, A.L.; Miao, S. Preparation, structure-property relationships and applications of different emulsion gels: Bulk emulsion gels, emulsion gel particles, and fluid emulsion gels. *Trends Food Sci. Technol.* **2020**, *102*, 123–137. [CrossRef]
190. Neves, B.S.; Gonçalves, R.C.; Mano, J.F.; Oliveira, M.B. Controlling the diffusion of small molecules from matrices processed by all-aqueous methodologies: Towards the development of green pharmaceutical products. *Green Chem.* **2023**, *26*, 4417–4431. [CrossRef]
191. Centurion, F.; Basit, A.W.; Liu, J.; Gaisford, S.; Rahim, M.d.A.; Kalantar-Zadeh, K. Nanoencapsulation for Probiotic Delivery. *ACS Nano* **2021**, *15*, 18653–18660. [CrossRef] [PubMed]
192. Li, M.; He, X.; Zhao, R.; Shi, Q.; Nian, Y.; Hu, B. Hydrogels as promising carriers for the delivery of food bioactive ingredients. *Front. Nutr.* **2022**, *9*, 1006520. [CrossRef] [PubMed]
193. Capuano, E.; Janssen, A.E.M. Food Matrix and Macronutrient Digestion. *Annu. Rev. Food Sci. Technol.* **2021**, *12*, 193–212. [CrossRef] [PubMed]
194. Fei, Y.; Ma, Y.; Zhang, H.; Li, H.; Feng, G.; Fang, J. Nanotechnology for research and treatment of the intestine. *J. Nanobiotechnology* **2022**, *20*, 430. [CrossRef] [PubMed]
195. Rahmati, F. Engineering probiotic delivery with nanocarriers: Overcoming gastrointestinal barriers and unlocking therapeutic potential: A review. *Biosci. Nanotechnol.* **2026**, *2*, 10. [CrossRef]
196. Tan, Y.; McClements, D.J. Plant-Based Colloidal Delivery Systems for Bioactives. *Molecules* **2021**, *26*, 6895. [CrossRef] [PubMed]
197. Yao, M.; Xie, J.; Du, H.; McClements, D.J.; Xiao, H.; Li, L. Progress in microencapsulation of probiotics: A review. *Compr. Rev. Food Sci. Food Saf.* **2020**, *19*, 857–874. [CrossRef] [PubMed]
198. Han, J.; McClements, D.J.; Liu, X.; Liu, F. Oral delivery of probiotics using single-cell encapsulation. *Compr. Rev. Food Sci. Food Saf.* **2024**, *23*, e13322. [CrossRef] [PubMed]
199. Kongprayoon, A.; Ross, G.M.; Limpeanchob, N.; Mahasaranon, S.; Punyodom, W.; Topham, P.D.; Ross, S. Bio-derived and biocompatible poly(lactic acid)/silk sericin nanogels and their incorporation within poly(lactide-co-glycolide) electrospun nanofibers. *Polym. Chem.* **2022**, *13*, 3343–3357. [CrossRef]
200. Maurya, V.K.; Shakya, A.; McClements, D.J.; Srinivasan, R.; Bashir, K.; Ramesh, T.; Lee, J.; Sathiyamoorthi, E. Vitamin C fortification: Need and recent trends in encapsulation technologies. *Front. Nutr.* **2023**, *10*, 1229243. [CrossRef] [PubMed]

201. Corredig, M.; Millqvist-Fureby, A.; Hansson, H.; Jackson, A.; Langton, M.; Maric, S.; Nordell, E.; Nylander, T.; Ladd-Parada, M.; Risbo, J.; et al. Boosting structural food science using X-ray and neutron techniques. *Food Hydrocoll.* **2025**, *170*, 111674. [CrossRef]
202. McClements, D.J.; Großmann, L. The science of plant-based foods: Constructing next-generation meat, fish, milk, and egg analogs. *Compr. Rev. Food Sci. Food Saf.* **2021**, *20*, 4049–4100. [CrossRef] [PubMed]
203. Vilgis, T.A. Gels: Model systems for soft matter food physics. *Curr. Opin. Food Sci.* **2015**, *3*, 71–84. [CrossRef]
204. Ribeiro, E.F.; Morell, P.; Nicoletti, V.R.; Quiles, A.; Hernando, I. Protein- and polysaccharide-based particles used for Pickering emulsion stabilisation. *Food Hydrocoll.* **2021**, *119*, 106839. [CrossRef]
205. Bochenek, S.; Camerin, F.; Zaccarelli, E.; Maestro, A.; Schmidt, M.M.; Richtering, W.; Scotti, A. In-situ study of the impact of temperature and architecture on the interfacial structure of microgels. *Nat. Commun.* **2022**, *13*, 3744. [CrossRef] [PubMed]
206. Wu, M.; Wang, H.; Lin, H.; Zhou, F.; Hou, G.; Miao, S.; Zheng, B.; Zhang, L. SPI/HG composite microgels with tunable structure and rheological properties for semi-solid foods. *Int. J. Biol. Macromol.* **2026**, *347*, 150682. [CrossRef] [PubMed]
207. Wang, Y.; Chai, J.; Shao, J.; Xu, X.; Zhao, X. Meat protein microgels assembled under various temperature-concentration conditions: Underlying its interfacial behavior. *Food Chem.* **2025**, *495*, 146211. [CrossRef] [PubMed]
208. Dyglė, G.; Eisinaitė, V.; Damulevičienė, G.; Leskauskaitė, D. Agar-collagen fluid gels as a dysphagia food: Rheological characterization vs fiberoptic endoscopic evaluation of swallowing. *Lith. Univ. Health Sci.* **2025**, *339*, 149776. [CrossRef] [PubMed]
209. Kim, S.J.; Kim, D.Y.; Jeong, D.; Lee, C.; Cho, H.-D.; Kim, M.P. Food-Grade Microgels for Age-Related Macular Degeneration: Design, Fabrication, and Targeted Delivery. *Gels* **2026**, *12*, 252. [CrossRef] [PubMed]
210. Zhang, J.; Liu, B.; Xie, Q.; Wang, J.; Li, M.; Yang, C.; Yang, X.; Guo, L.; Su, Y.; Jiang, Y. Polysaccharide-based microgels for probiotic delivery: Advances in design, fabrication, and functional food applications. *Trends Food Sci. Technol.* **2026**, *170*, 105621. [CrossRef]
211. Wal, A.; Bukke, S.P.N.; Vidiyala, N.; Jamil, S.; Sharma, K.K.; Khan, A.; Dutta, A.; Sunkishala, P.; Gasmi, A. Stimuli-responsive nanogels as intelligent nanocarriers for tumor microenvironment-triggered anticancer drug delivery. *Discov. Nano* **2026**, *21*, 247. [CrossRef] [PubMed]
212. Terziyska, M.; Vladev, V.; Terziyski, Z.; Ilieva, I.; Bozhkov, S. Application of peptide nanostructures in the food industry. *BIO Web Conf.* **2025**, *170*, 01002. [CrossRef]
213. Machado, M.; Costa, E.M.; Silva, S. Soft Gels in Food Systems: Recent Advances, Applications, and Technological Innovations. *Gels* **2025**, *11*, 667. [CrossRef] [PubMed]
214. Madadlou, A. Liquid–liquid phase separation as a structuring tool for designing anisotropic food systems. *Soft Matter* **2025**, *22*, 2780–2792. [CrossRef] [PubMed]
215. Ke, Q.; Zhang, J.; Huang, X.; Kou, X.; Zhang, D. Machine learning unveils three layers of food complexity. *npj Sci. Food* **2026**, *10*, 87. [CrossRef] [PubMed]
216. Lee, D.; Jeong, S.; Yun, S.; Lee, S. Artificial intelligence-based prediction of the rheological properties of hydrocolloids for plant-based meat analogues. *J. Sci. Food Agric.* **2024**, *104*, 5114–5123. [CrossRef] [PubMed]
217. Dahl, J.F.; Schlangen, M.; van der Goot, A.J.; Corredig, M. Predicting rheological parameters of food biopolymer mixtures using machine learning. *Food Hydrocoll.* **2024**, *160*, 110786. [CrossRef]
218. Tabatabaei, Z.; Soto Aguilar, D.; Bonilla, J.C.; Clausen, M.P.; Sporring, J. Topological texture analysis of microscopy images of dynamic casein gelation and its relation to rheological properties. *arXiv* **2026**, arXiv:2606.02048. [CrossRef]
219. Wong, K.; Arruda, T.R.; Butler, K.T.; Guldin, S.; Schrettl, S. Machine learning for food colloids: Novel tools to advance fundamental understanding, stability, texture, and processability. *Curr. Opin. Colloid Interface Sci.* **2025**, *78*, 101937. [CrossRef]
220. Siddique, A.; Gupta, A.; Sawyer, J.T.; Huang, T.; Morey, A. Big data analytics in food industry: A state-of-the-art literature review. *npj Sci. Food* **2025**, *9*, 36. [CrossRef] [PubMed]
221. Top, J.L.; Janssen, S.; Boogaard, H.; Knapen, R.; Şimşek-Şenel, G. Cultivating FAIR principles for agri-food data. *Comput. Electron. Agric.* **2022**, *196*, 106909. [CrossRef]
222. Basak, S.; Singhal, R.S. The potential of supercritical drying as a "green" method for the production of food-grade bioaerogels: A comprehensive critical review. *Food Hydrocoll.* **2023**, *141*, 108738. [CrossRef]
223. Manzocco, L.; Mikkonen, K.S.; García-González, C.A. Aerogels as porous structures for food applications: Smart ingredients and novel packaging materials. *Food Struct.* **2021**, *28*, 100188. [CrossRef]
224. Yashini, M.; Ci, H.; Sheeba, K.N.; Kumar, P.S. Valorization of Agro-industrial Wastes into Cellulose Gels for Food Applications: A Review of Recent Advances. *Food Bioprocess Technol.* **2026**, *19*, 111. [CrossRef]
225. Baudron, V.; Gurikov, P.A.; Smirnova, I.V.; Whitehouse, S. Porous Starch Materials via Supercritical- and Freeze-Drying. *Gels* **2019**, *5*, 12. [CrossRef] [PubMed]
226. Ciftci, D.; Ubeyitogullari, A.; Huerta, R.R.; Ciftci, O.N.; Flores, R.A.; Saldaña, M.D.A. Lupin hull cellulose nanofiber aerogel preparation by supercritical CO2 and freeze drying. *J. Supercrit. Fluids* **2017**, *127*, 137–145. [CrossRef]
227. Wang, Z.; Zhu, W.; Huang, R.; Zhang, Y.; Jia, C.; Zhao, H.; Chen, W.; Xue, Y. Fabrication and Characterization of Cellulose Nanofiber Aerogels Prepared via Two Different Drying Techniques. *Polymers* **2020**, *12*, 2583. [CrossRef] [PubMed]

228. Manzocco, L.; Plazzotta, S.; Powell, J.A.; de Vries, A.; Rousseau, D.; Calligaris, S. Structural characterisation and sorption capability of whey protein aerogels obtained by freeze-drying or supercritical drying. *Food Hydrocoll.* **2021**, *122*, 107117. [CrossRef]
229. Mißfeldt, F.; Gurikov, P.A.; Lölsberg, W.; Weinrich, D.; Lied, F.; Fricke, M.; Smirnova, I.V. Continuous Supercritical Drying of Aerogel Particles: Proof of Concept. *Ind. Eng. Chem. Res.* **2020**, *59*, 11284–11295. [CrossRef]
230. Tom, C.; Sangitra, S.N.; Pujala, R.K. Rheological fingerprinting and applications of cellulose nanocrystal based composites: A review. *J. Mol. Liq.* **2023**, *370*, 121011. [CrossRef]

Disclaimer/Publisher's Note: The statements, opinions and data contained in all publications are solely those of the individual author(s) and contributor(s) and not of MDPI and/or the editor(s). MDPI and/or the editor(s) disclaim responsibility for any injury to people or property resulting from any ideas, methods, instructions or products referred to in the content.